

Contents

Contents	i
1 Patterns of sitewise selection in mammalian genomes	2
1.1 Introduction	2
1.2 The Mammalian Genome Project	3
1.3 Data quality concerns: sequencing, assembly and annotation error	4
1.3.1 The impact of sequencing errors on error rates in detecting positive selection	4
1.3.2 Filtering out low-quality sequence	10
1.3.3 Removing recent paralogs	12
1.3.4 Identifying clusters of non-synonymous substitutions	18
1.4 Genome-wide analysis of sitewise selective pressures in mammals	22
1.4.1 Species groups for sitewise analysis	22
1.4.2 Evaluation of the bulk distributions and the design of a filtering approach	27
1.4.3 The global distribution of sitewise selective pressures in mammals	34
1.4.3.1 Site patterns and ω_{ML} values reveal the prevalence of purifying selection in mammalian proteins	34
1.4.3.2 Sitewise confidence intervals and LRT statistics identify sites with significant evidence for purifying and positive selection	36
1.4.4 Modeling the global distribution of sitewise selective pressures	41
1.4.5 Simulations to evaluate the power to detect positive selection and estimate selective pressures	43

CONTENTS

1.4.6	Evaluation of the effect of GC content, recombination rate, and codon usage on sitewise dN/dS estimates and the detection of positive selection	43
1.5	Conclusions	51
	Bibliography	53

CONTENTS

length ratio windows of clustered substitution

Chapter 1

Patterns of sitewise selection in mammalian genomes

1.1 Introduction

This chapter describes the use of sitewise evolutionary estimates to characterize the global distribution of selective constraint across 38 mammalian genomes and within the major mammalian superorders. I will apply the Sitewise Likelihood Ratio (SLR) test, evaluated in Chapter ??, to the set of mammalian orthologous gene trees from Chapter ?? to generate genome-wide sets of sitewise statistics measuring selective constraint in several groups of mammalian species. Both this chapter and the following one are concerned with the analysis of these data: here I will consider the overall distribution of constraint observed in each set of genomes, while Chapter ?? will look at the application of sitewise data to identify gene- and domain-centric evolutionary trends.

I will first introduce the scientific context of this project—namely, the sequencing and analysis of several mammalian genomes for the Mammalian Genome Project (MGP)—and outline the main questions motivating the analysis I performed.

The next section describes the preparation and alignment of the mammalian gene tree from Chapter ?? and introduce a protocol for filtering genome-wide sitewise estimates. Although the simulations from Chapter ?? showed that sequences with divergence levels above that of most mammalian proteins can be aligned without introducing many false positives due to misaligning biological insertions and deletions, the analysis of empirical sequence data involves many potential non-evolutionary sources of alignment error. A sequenced and annotated genome is not a piece of observed data; rather, it is the result of

a succession of inferences (based ultimately on the observation of a pool of genomic DNA by some sequencing technology), each step along the way involving potential errors and biases. Chapter ?? looked at the identification of mammalian orthologs, showing that the inference of correct gene tree structures is fraught with difficulty and that low-coverage genomes are under-represented in gene duplications. Other sources of error, including those occurring while reading DNA bases [TOCITE, 2011], assembling genomic fragments [TOCITE, 2011], and annotating gene-coding regions [TOCITE, 2011] have all been previously highlighted as being important in the large-scale analysis of genomic data. As such, care was taken to design and evaluate a variety of filters to reduce the probability of yielding misleading results.

The third part of this chapter characterizes the global distribution of mammalian selective constraint in three ways: first, using the SLR statistic to identify sites evolving under purifying and positive selection at various confidence levels; second, fitting parametric distributions to the set of sitewise estimates to infer the distribution of selective pressures; and third, evaluating the impact of genomic variation in GC content and recombination rate on the distribution of sitewise estimates.

1.2 The Mammalian Genome Project

A major goal of mammalian comparative genomics has been to quantify, identify and understand the fraction of the human genome that is under evolutionary constraint. The first non-human mammalian genomes showed at least 5% of the human genome to be under purifying selection [Lindblad-Toh *et al.*, 2005; Mouse Genome Sequencing Consortium & Mouse Genome Analysis Group, 2002; Rat Genome Sequencing Project Consortium, 2004], but the small number of genomes available limited the extent to which regions of evolutionary constraint could be identified. The Mammalian Genome Project, a coordinated set of genome sequencing projects initiated in 2005 and organised by the Broad Institute of MIT and Harvard, was designed with the primary purpose of increasing the accuracy and confidence with which regions of the human genome that have evolved under evolutionary constraint in mammals could be identified [Margulies *et al.*, 2007]. In line with this goal, 20 mammalian species were chosen for sequencing in order to maximise the amount of evolutionary divergence available for comparative analysis when combined with the 9 already available sequenced genomes [Margulies *et al.*, 2005]. Most of the 20 additional species were only sequenced to a target twofold coverage, meaning each genomic base pair

would be covered on average by two sequence reads and roughly 85% of genomic sequence would be covered by at least one read. The decision to sequence many genomes at low coverage was a deliberate choice, designed to maximize the average amount of branch length available for the identification of constrained sequence [Margulies *et al.*, 2007].

As the Mammalian Genome Project proceeded from its sequencing to analysis phase in late 2008, it was clear that the additional branch length afforded by the 29-species phylogeny would enable a number of evolutionary analyses beyond the identification of constrained non-coding regions. These included the evolutionary characterisation of gene promoters, identification of exapted non-coding elements, detection of evolutionary acceleration and deceleration in non-coding regions, and detection of purifying and positive selection in protein-coding genes. Given the prior involvement of the Goldman group in analysing the ENCODE comparative sequencing data [ENCODE Project Consortium, 2007; Margulies *et al.*, 2007] and Tim Massingham’s development of the SLR software for sitewise evolutionary analysis [Massingham & Goldman, 2005], the group was recruited to perform the protein-coding evolutionary analysis for the Mammalian Genome Project, and the project turned into a portion of my PhD research. This chapter describes my work on the project, which began in late 2008; all of the work described below was performed by me, though I benefitted greatly from advice and discussion with members of the Goldman group (Nick Goldman and Tim Massingham), the Ensembl Compara team (Albert Vilella, Javier Herrero, Ewan Birney) and the organisers and members of the Mammalian Genome Project (especially Manolis Kellis, Kerstin Lindblad-Toh, Mike Lin, and, Katie Pollard). The major results from the initial version of this analysis have recently been published [Lindblad-Toh *et al.*, 2011]; the work presented below includes some improvements to the filtering and alignment methodology and incorporates sequence data from a number of genomes which were restricted from use in the Mammalian Genome Project analysis.

1.3 Data quality concerns: sequencing, assembly and annotation error

1.3.1 The impact of sequencing errors on error rates in detecting positive selection

The possibility that erroneously-aligned sequences might cause false positives in the detection of sitewise positive selection was a major concern for this analysis, especially given

the low-coverage nature of the 20 newly-sequenced genomes. Although the SLR test and other sitewise maximum likelihood methods have been shown to be conservative in their identification of positively selected sites under most conditions, even when the amount of data is low or the null model is violated [Anisimova *et al.*, 2002, 2003; Massingham & Goldman, 2005], most evolutionary analyses are based on the assumption that all sites within an alignment column are truly homologous. This assumption can be violated in a number of ways, some of which are described below.

Of course, alignment error can result from errors in reconstructing the evolutionary history of sequences evolving with indels, causing non-homologous codons to be placed in the same alignment column. In Chapter ?? I explored the tendency of a number of progressive multiple alignment programs to produce such errors, showing that PRANK_C alignments introduce few falsely identified positively-selected sites resulting from alignment errors at mammalian-like divergence levels. Thus, PRANK_C was used to align all coding sequences, and the number of false positives resulting from misalignment of biological insertions and deletions was expected to be low.

However, biological indels are not the only potential source of misalignment error. Errors resulting from the inclusion of incorrect genomic sequence in coding sequences were an additional concern. Twenty of the genomes under study were sequenced at low coverage and were not assembled into chromosomes or finished to completion, making the likelihood of miscalled bases, spurious insertions or deletions, or shuffled regions due to mis-assembly relatively high [Green, 2007]. The magnitude of the effect of each of the aforementioned types of sequence errors on the detection of positive or purifying selection depends on the nature of the inference method, the type of sequencing error, and the branch length of the terminal lineage leading to the species containing the sequence error.

As most codon-based inference methods assume independence between amino acid sites, the effect of misalignment on the resulting inference will be independent between neighboring codons. Thus, one may first consider the effect—in isolation—of a single spuriously-assigned homologous codon on the maximum likelihood estimation of ω . Two distinct situations can be encountered: first, the case where a single sequence error causes one spurious nucleotide substitution within a codon, and second, the case where one or multiple sequence or assembly errors cause multiple spurious substitutions within a codon. Single spurious nucleotides, such as miscalled bases, would add noise to the estimation of ω , but as a whole they would not be expected to cause false positive positively selected codons. If we assume no large difference between the natural mutational process and the process that

caused the erroneous mutation (e.g., a random distribution across codon positions and no bias in the identity of the miscalled base) then the effect would be to shift the estimated ω in the branch containing the error towards 1. This is because, on average, isolated miscalled bases would appear the same as a neutral substitution process, inflating the estimated substitution rate but not affecting the relative non-synonymous and synonymous rates.

In contrast to single spurious substitutions, codons with multiple erroneous bases in one species may produce strongly elevated inferred substitution rates and ω estimates. This is due to the necessity of the codon model implemented in SLR to infer a multi-step path of single substitutions between the two codons on either side of a given evolutionary branch. The exact maximum likelihood path estimated between two completely non-homologous codons depends on the estimated codon frequencies, the branch length separating the two sequences, and the nature of the process causing misalignment of nonhomologous codons, but in general it would be reasonable to expect a greater number of false positive PSSs resulting from codons with multiple erroneous bases than from codons with single errors due to the necessary inference of a multi-step path between codons with multiple nucleotide differences.

Given the potentially greater impact of codons with multiple errors, the propensity of each of the common sequencing error types identified above (miscalled bases, spurious indels, and shuffled/repeated/collapsed regions due to mis-assembly) to cause single or multiple errors within codons could strongly affect its impact on the sitewise detection of positive selection. On its own, a miscalled nucleotide base would obviously result in a single spurious substitution. However, low-quality bases tend not to be uniformly distributed among or within sequence reads [Kircher *et al.*, 2009], increasing the probability of multiple errors within a codon resulting from miscalled bases. Spurious indels within coding regions may be even more likely than miscalled bases to cause multiple errors within a codon due to the potential for creating frameshift artifacts. Assembly errors, which result in larger-scale structural errors including missing, repeated, shuffled or inverted sequence regions [Jaffe *et al.*, 2003], are especially prone to producing codons with multiple erroneous substitutions due to the large amount of contiguous sequence data being misplaced.

For detecting positive selection, the nature of the model used for inferring positive selection and the branch lengths separating the species being tested may also have an impact on the prevalence false positives resulting from sequence errors. Sequence errors should only substantially affect the estimation of non-synonymous and synonymous substitution

rates along the terminal lineage leading to the erroneous sequence data; thus, the potential impact of sequencing error on the inference of a positively selected site or gene can be estimated by considering the potential impact of an inflated rate of non-synonymous substitution along the terminal branch on the inference of positive selection with a given test. Both the branch-site test for positive selection (which is not used in this analysis) and the sitewise tests for positive selection (including PAML M8 and SLR, first described in Chapter ??) are sensitive to erroneous substitutions occurring at individual alignment columns, with the major difference between the two types of test being that the branch-site test is highly sensitive to substitutions along the foreground branch(es) being tested for positive selection, while sitewise tests only measure the signal for positive selection across the entire evolutionary tree.

For the branch-site test, the potential effect of sequencing error should depend on the location and length of the foreground branch(es): if the terminal branch leading to the spurious sequence is within the foreground, and especially if it represents a sizeable portion of the overall foreground branch length, then false positives could easily result; if, however, the terminal branch is outside of the foreground, then it would have little direct impact on the FPR of the branch-site test aside from adding noise to the estimation of parameters in the non-foreground branches of the tree.

For site-based tests such as SLR, the effect of sequencing error should be independent of the position of the terminal branch within the tree, depending more on the magnitude of non-synonymous substitution rate elevation resulting from the sequence error and the fraction of total branch length covered by the “erroneous” terminal branch within the phylogenetic tree being studied. It would be difficult to consider each of these factors (the terminal branch length and the magnitude of non-synonymous substitution rate elevation) in isolation due to their non-independence: sequence errors in a short terminal branch may yield a strongly elevated non-synonymous substitution rate, but the impact on the overall inference of positive selection may be limited as a result of the short branch length. On the other hand, the same erroneous sequence in a species with a longer terminal branch would likely cause a smaller elevation in the non-synonymous substitution rate (due to the higher expected number of substitutions along a longer branch) yet the impact of such an elevated rate on the sitewise inference would be proportionally greater due to the higher branch length. A reasonable hypothesis would be that these opposing factors would effectively cancel each other out in the maximum likelihood calculations. In either case, the expectation that a phylogeny with a greater proportion of its branch length

within terminal branches (which, in contrast to internal branches, may contain spurious substitutions resulting from sequencing errors) would be more prone to false positives should still hold.

To summarize, the expected effect of alignment errors on the sitewise detection of positive selection should be minimal when using a good aligner and analysing data within vertebrate divergence levels, but the number of false positives resulting from sequence errors depends on a number of factors including the frequency, spatial clustering, and terminal branch length associated with sequencing, assembly and annotation errors. In some cases, even a relatively large amount of sequencing error may not produce a strongly elevated FPR (e.g., when the total internal branch length is large as when analyzing all mammals or vertebrates), as the addition of a few spurious substitutions would not significantly change the estimated non-synonymous substitution rate. In other cases, however (e.g., when the branch length is small, and/or many low-quality genomes are included), it may significantly bias results towards excess false positives.

Simulation studies similar to those I performed in Chapters ?? and ?? could improve our understanding of the relative potential of different types of sequencing errors to introduce false positives in downstream analyses, but the absolute frequency and pattern of such errors would still be difficult to predict without a reliable model for their generation. This is especially true for larger-scale errors from misassembly or misannotation, which are less easily modeled than base calling errors and could have potentially more significant negative effects. Instead, an empirical approach seems more appropriate for quantifying the false positives resulting from these types of sequence errors. In particular, two empirical studies in mammals have provided convincing evidence that sequence, alignment and annotation errors can drastically increase the number of false positive PSGs in the branch-site test for positive selection.

Schneider et al. [2009] performed a genome-wide scan for positive selection in the terminal branches of 7 mammalian genomes using the branch-site test and analysed the fraction of PSGs within subsets of high- or low-quality genes according to three sequence and alignment quality metrics. They found that the fraction of PSGs was significantly higher for genes exhibiting lower quality sequence, annotation and alignment metric, with genes in the highest-quality and lowest-quality categories showing a 7.2-fold difference in the inferred fraction of PSGs [Schneider *et al.*, 2009]. This observation provided evidence of a correlation between the chosen quality metrics and the tendency of an alignment to exhibit positive selection. It did not necessarily imply causation, however, as the same

result might have been observed—even in the absence of sequence error—if some biological properties of the true PSGs caused them to yield lower quality metrics than non-PSGs. Looking at the three metrics used in their study (sequencing coverage, gene annotation status, and alignment quality according to the heads-or-tails method), it is plausible that properties associated with elevated ω ratios and positive selection, such as recent gene duplication [Beisswanger & Stephan, 2008; Casola & Hahn, 2009; Studer *et al.*, 2008], high GC content [Ratnakumar *et al.*, 2010] or functional shifts [Storz *et al.*, 2008; Wang & Gu, 2001] might have had an error-independent effect resulting in a higher proportion of PSGs in low-scoring categories. The heads-or-tails method has also been shown to be inappropriate for estimating alignment uncertainty [Fletcher & Yang, 2010], so results based on this measurement should be taken with caution. Despite these criticisms, the analysis did provide good evidence that some of the obvious sources of error may be contributing to excessive estimates of branch-specific positive selection in mammals.

Mallick *et al.* [2009] took a different approach to the same problem by performing a careful resequencing and reassembly of the chimpanzee genome (the initial assembly of which had lower coverage and lower quality than the human genome) and re-analysing the evidence for positive selection along the chimpanzee lineages in 59 genes which had previously been identified as chimpanzee PSGs. The authors, who were motivated by a concern that previous reports of a larger proportion of PSGs in chimpanzee than in human [Bakewell *et al.*, 2007] were the result of its lower-quality genome rather than a biologically significant difference in levels of adaptation, found that the vast majority of PSGs identified in two previous studies showed no evidence for positive selection when using their reassembled and higher-coverage version of the chimpanzee genome [Mallick *et al.*, 2009]. This suggested that the original 4x coverage chimpanzee genome contained a number of sequencing and assembly errors leading to false inferences of positive selection. A detailed analysis of 302 codons with multiple spurious non-synonymous substitutions in the original assembly showed roughly comparable effects of sequence error (explaining 23% of codons), assembly error (14% of codons) and local alignment error (30% of codons).

Taken together, the results of Schneider *et al.* [2009] and Mallick *et al.* [2009] provide strong evidence in support of the hypothesis that errors in sequencing, assembly, annotation and alignment can result in strongly elevated inferred ω values when using sensitive tests for detecting positive selection. Furthermore, the detailed identification and quantification of error sources performed by Mallick *et al.* [2009] provided an empirical estimate of how important each potential source of error would be in the detection of positive selection.

Although both of these studies used the branch-site test for detecting positive selection, their results could be expected to generalize well enough to guide the design of filtering methods for the present sitewise analysis. With this work in mind, I implemented three filtering steps to help identify and remove sequences and alignment regions potentially subject to the errors noted above: filtering out low-quality sequence, removing gene fragments and recent paralogs, and identifying alignment regions with extremely high numbers of clustered substitutions.

1.3.2 Filtering out low-quality sequence

Due to the presence of several low-coverage genome assemblies in the set of available mammalian genomes and the elevated sequencing error rates in such assemblies [Hubbard *et al.*, 2007], I applied a conservative filter to the set of input sequences based on sequence quality scores where available.

Most automated genome assembly pipelines, such as the Arachne tool used to sequence many of the low-coverage mammalian genomes [Jaffe *et al.*, 2003], output a set of Phred quality scores alongside the identified genome sequence, with one Phred score per base ranging in value from 0 to 50. A Phred score represents the probability, calculated by the sequencing and/or assembly program, that a given base call is incorrect. This probability is usually concisely expressed as the negative logarithm of the probability of an error multiplied by ten, or $Q = -10\log_{10}P$, where Q is the Phred score and P is the probability of an incorrect base call [Cock *et al.*, 2010].

Although Ensembl was used as the source for gene sequences in this analysis, it does not store quality scores from its source genome assemblies, so Phred quality scores were manually downloaded for all genomes with Phred-like quality scores made publicly available alongside the genomic sequence. Most quality scores were provided as a single file in FASTA format with one string of numerical scores per assembled contig. Since the process of filtering a single mammalian coding alignment required collecting scores from many different quality score files for many disjoint genomic locations, a custom script was written to process each quality score file to allow for faster score retrieval and better memory performance. In total, quality score files for XYZ genomes were indexed and used for quality filtering.

A suitable score threshold for filtering coding regions was chosen based on a study by Hubisz *et al.* [2011], who performed a detailed analysis of Phred quality scores, which are a probabilistic prediction of the error rate, and actual error rates in low-coverage mammalian

genome assemblies by comparing the low-coverage assemblies to matched regions of high-quality sequence from the ENCODE comparative genomics dataset [ENCODE Project Consortium, 2007]. The authors identified a strong correlation between Phred scores and actual error rates for scores below 25, indicating that the scores were accurate predictors of the true error rate in this range. Error rates did not decrease significantly at scores above 25, however, suggesting that the use of an extremely high Phred score threshold would only minimally reduce error levels below those obtained with a moderate threshold. Furthermore, Hubisz et al. noted that 85% of bases in the low-coverage mammalian genomes contain very high Phred scores (> 45) and only 4% have low scores (< 20).

Based on these observations, a threshold Phred score of 25 was chosen as a reasonable trade-off between the potential benefit of avoiding miscalled bases and the potential cost of masking out correctly sequenced bases. For each protein-coding sequence with quality scores available, a “minimum score” approach was used to filter out whole codons: all codons containing one or more nucleotides with a score below 25 were masked out with three ambiguous nucleotides, 'NNN'.

The expected proportion of filtered nucleotides could be calculated from the fraction of bases below the Phred score threshold of 25. According to Hubisz et al. [2011], approximately 5% of bases in low-coverage mammalian genomes contain Phred scores below 25. The worst case scenario (e.g., the worst case in terms of the number of high-quality bases being masked as a result of using the minimum score approach) would be if only one base per codon had a score below the threshold. In that case, an expected 15% of nucleotides would be filtered, since 3 bases would be masked for every low-quality base. However, the distribution of low-quality bases is likely highly clustered, due to the uneven distribution of repetitiveness and GC content as well as the tendency for uncertain base calls to occur towards the end of sequence reads (all of which are known to affect read coverage and assembly performance, e.g. Teytelman *et al.* [2009]). A more clustered distribution of low-quality bases would cause fewer high-quality bases to become masked by the minimum score approach, reaching the limit of an expected 5% total filtered bases if low-quality bases always occurred in groups of three and were positioned along the boundary of codon triplets. Thus, anywhere from 5% to 15% of nucleotides from low-coverage genomes were expected to be filtered by this approach.

The above filtering scheme was applied to all coding sequences from each species for which quality scores were available, which included all of the species with low-coverage genomes as well as five with high-coverage genomes: chimpanzee, guinea pig, dog, horse,

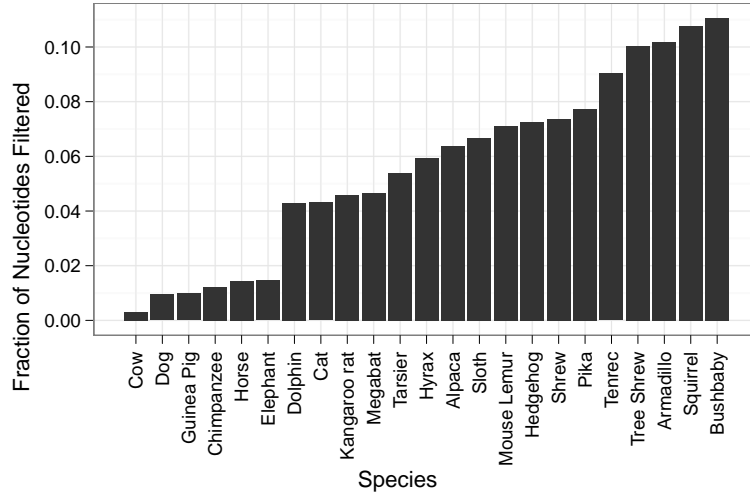


Figure 1.1

cow, and elephant. (Note that guinea pig and elephant genomes were originally sequenced at low 2x coverage for the MGP, but they have since undergone additional sequencing to produce high-coverage 7x assemblies. These assemblies were used in Ensembl version 63 and thus in the analysis described below.) The overall percentage of nucleotides filtered from each genome is shown in Figure 1.1. As expected, genomes with high-coverage sequences contained fewer bases with low Phred scores, resulting in 1-2% of nucleotides being filtered. The bulk of low-coverage genomes resulted in 4-8% of nucleotides being filtered, while five genomes (bushbaby, squirrel, tree shrew, armadillo and tenrec) showed a noticeably higher proportion of low-quality bases, with 9-11% nucleotides being filtered out. The distribution of filtered nucleotide proportions confirmed the expectation that 5-15% of nucleotides would be filtered using a Phred score threshold of 25, and the variation in filtered nucleotide proportions between different species showed that despite the uniform 2x coverage of the low-coverage mammalian genomes, different assemblies varied widely in their distributions of sequence quality scores within coding regions.

1.3.3 Removing recent paralogs

As discussed in Section ??, the inclusion of paralogous gene relationships in a large-scale analysis of orthologous gene evolution may produce misleading signals of adaptive evolution [Lynch & Conery, 2000], artifacts resulting from gene conversion [TOCITE, 2011], and produce biases due to lineage-specific family expansion, a process which is relatively

common in mammalian gene families [TOCITE, 2011]. As a result, it has traditionally been considered important to filter out recently-duplicated genes (e.g., genes duplicated after the whole-genome duplication event in the vertebrate ancestor) in large-scale evolutionary analyses. Previous genome-wide scans for positive selection involving six or fewer mammalian genomes have either required strict one-to-one orthology [Clark *et al.*, 2003; Nielsen *et al.*, 2005] or allowed very limited numbers of recent duplications in specific lineages [Kosiol *et al.*, 2008]. With larger mammalian trees, however, the requirement of strict one-to-one orthology becomes increasingly untenable: if gene duplications and deletions occur randomly in time, then the probability of observing at least one such event in a given gene family should increase linearly with the amount of branch length covered by the tree. The requirement of one-to-one orthology would result in fewer genes being available for analysis as more species are incorporated into the analysis, which is clearly an undesirable trend. As an alternative to ignoring genes which do not satisfy the requirement of strict orthology, I developed an approach, described below, for handling recently duplicated genes by removing the more-divergent paralogous copy from the the gene tree.

Before describing the method for duplications, it is worth making a point about gene deletions. Specifically, I note that gene deletions can cause problems in the branch-specific detection of positive selection, but they should not have a detrimental effect on tests for selection across the entire tree. The branch-specific effect of a gene deletion results from the merging of multiple ancestral branches into one. Take for example the inference of mutations along the evolutionary tree of human, chimpanzee and gorilla, which contains two internal nodes: *HC*, the human-chimpanzee ancestor, and *HCG*, the human-chimpanzee-gorilla ancestor. When sequences from all species are present, mutations can be separately identified as occurring along the branch from *HCG* to *HC* and along the branch from *HC* to the human sequence, allowing for a test to differentiate between a signal of adaptive evolution in one branch or the other. For a gene which was deleted in chimpanzee those two branches become effectively merged into one, and mutations can only be inferred to have occurred between *HCG* and the human sequence. The time-specificity of estimated evolutionary rates is thus reduced, and when the identity of the branch along which synonymous and non-synonymous mutations have occurred is important to a test for positive selection, this difference can complicate the interpretation of results. Acknowledging this effect, Kosiol *et al.* [2008] used a different set of orthology requirements for each branch-specific test for positive selection performed. When the test for positive selection does not depend on the identity of specific branches in the tree, however, a gene deletion would only

serve to reduce the total amount of branch length available for inference. As long as the branch leading to the deleted species did not comprise a large portion of the total branch length, the effect of gene deletion on the results of tree-wide tests for selection should be minimal.

Turning back to gene duplications, an additional complicating factor in the current analysis was the concern that many of the apparent gene duplications were actually artifacts of the annotation of low-coverage genomes. Each low-coverage genome assembly is highly fragmented, meaning that it contains many short sequence segments that were unable to be assembled into chromosome-sized sequences due to missing sequence data. Sometimes the exons of a gene spanned the boundaries of these sequence segments, causing different parts of a gene to exist on different segments. The Ensembl annotation pipeline was not designed to merge gene annotations across different sequence segments, so each part of a gene residing on multiple sequence segments would be annotated as a separate shortened gene. These shortened genes would be treated as independent proteins by the Compara pipeline, likely being placed at very similar positions in the gene tree due to each sequence having been derived from a gene with a single correct evolutionary position. While this result might not be detrimental to sitewise analysis in itself (as each shortened gene might be correctly aligned and provide useful information to the alignment), a number of factors, including the low quality of genomic sequence and assembly within these shortened genes, problems with aligning small fractions of a gene against complete sequences, and the potential for incorrect placement of fragmented sequences within the gene tree, made it desirable to remove these shortened genes before estimating evolutionary rates. These split genes could be effectively identified by their shortened length.

Sequence divergence was the other criterion by which I selected which paralogous copy of recently-duplicated genes to retain for evolutionary analysis. A well-established theoretical model of evolution after gene duplication predicts that one of the duplicate copies retains the ancestral function (and its associated pattern of evolutionary constraint) while the other duplicate experiences relaxed constraint followed by either degradation or functional diversification [Han *et al.*, 2009]. Thus, the least-diverged copy of a recently duplicated gene should be the one most likely to have retained the pattern of evolutionary constraint shared among the mammalian species being examined in this study.

The protocol I implemented for filtering apparent paralogs used both gene length and sequence divergence to identify which gene among a set of apparent paralogous copies was most suitable to retain for sitewise analysis. Gene length was used primarily to discrim-

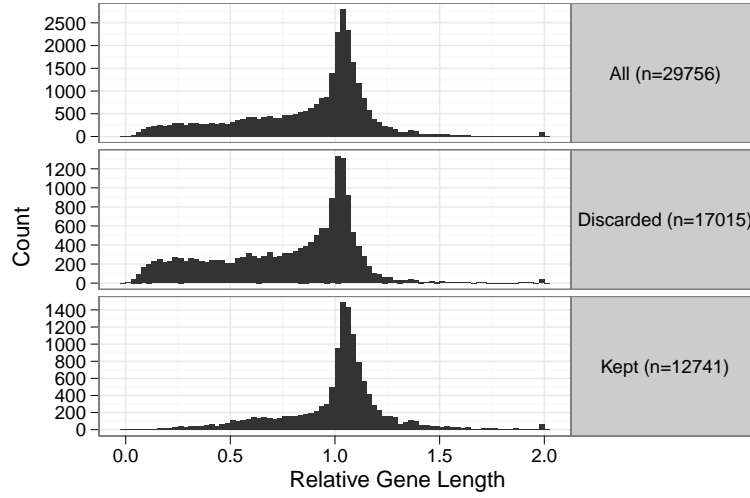


Figure 1.2: Length ratios of putative paralogs. The length ratio was calculated as the length of a putative paralogous copy divided by the mean length all sequences its corresponding gene tree. Putatively paralogous genes (top panel) were either discarded (middle panel) or kept (bottom panel) according to rules based on their length and mean sequence divergence from other aligned sequences, as described in the text.

inate spuriously shortened genes from true genes, and sequence divergence was used to distinguish between more- and less-diverged paralogs. First, the mean pairwise sequence distance was calculated between each putative paralog and all other sequences in the gene tree, resulting in one mean pairwise distance estimate per putative paralog (hereafter referred to as the mean distance). For these distance calculations, the stock Compara codon alignments and the JC69 nucleotide model to estimate distances. Second, the ratio of the sequence length of each putative paralog to the mean sequence length across the tree (hereafter referred to as the length ratio) was also calculated.

Genes were grouped by species within each gene tree, and any group of 2 or more genes was considered to be a set of putative paralogs. Within each set of putative paralogs, a single gene was chosen to be retained for evolutionary analysis based on three rules applied in the following order: (1) if only one sequence had a length ratio above 0.5 and all others had a length ratio below 0.5, the longest sequence was kept; (2) if at least one sequence yielded a mean distance below the others, that sequence was kept; (3) if all mean distances were identical then the longest sequence was kept, or if all mean distances and length ratios were equal, an arbitrary choice was made.

These rules were applied to each of the 29,756 putative paralogs contained within the 16,XYZ largely orthologous gene trees from the previous chapter. Figure 1.2 shows the

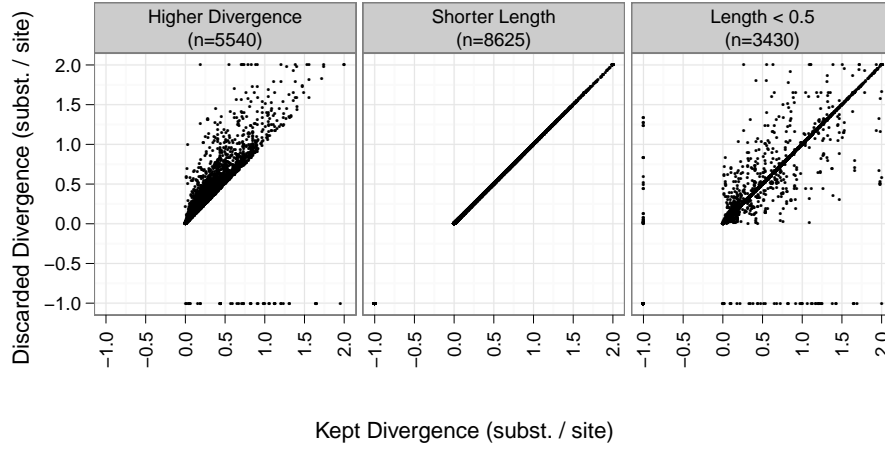


Figure 1.3: Sequence divergence of kept and discarded putative paralogs. Each point represents a gene which was discarded from the tree for one of three reasons: it had more sequence divergence than the kept gene (*Higher Divergence*; left panel), it had equal sequence divergence but shorter length than the kept gene (*Shorter Length*; middle panel), or it had a gene length (relative to the mean across all sequences) of less than 0.5 while the kept copy had a relative length greater than 0.5 (*Length < 0.5*; right panel). Divergence was measured as the mean pairwise divergence between the gene and all other sequences in the tree, and a value of -1 was assigned to genes for which no reliable divergence estimate could be attained due to a lack of sufficient data)

distributions of length ratios separately for the set of all putative paralogs, those discarded from the alignments, and those kept for subsequent analysis. The overall distribution of length ratios shows that most putative paralogs had lengths similar to the mean length across the gene tree (with a peak at or slightly above 1), but the shape of the distribution was asymmetric, with a strong bias towards shorter lengths. The filtering protocol effectively removed these shortened genes, as evidenced by the strong enrichment of lower length ratios in the distribution of discarded genes and the less skewed distribution of length ratios in the set of XYZ kept paralogs.

To better compare the characteristics of the discarded and kept genes, a more detailed view of the results of the paralog filter is presented in Figure 1.3, showing a scatter plot of the mean distance and length ratio of each discarded paralog compared to that of the corresponding kept paralog. Figure 1.3 is separated into panels according to the rule used to discard the paralogous copy: the first panel corresponds to rule (1), where genes with a length ratio below 0.5 were discarded; the second panel corresponds to rule (2), where genes with higher mean distances were removed; the third panel corresponds to rule (3),

where all genes had equal mean distances and the longest gene was kept (or, if all lengths were equal, an arbitrary choice was made).

The first panel of Figure 1.3 shows that genes discarded on the basis of having a very short length contained sequence distances similar to the kept copies, as the highest density is along the diagonal and there is no apparent bias for genes to lie above or below the diagonal. This is in line with the expectation that these discarded genes were not truly paralogous copies, but rather fragments of split genes resulting from unassembled sequence segments. The second panel shows that when paralogous copies could be differentiated by their mean distances, they tended to have low average distances (<0.5 substitutions per nucleotide site) and only a small difference between the kept and discarded copy (e.g., most of the distribution is just above the diagonal, and few points are above the dashed line with a slope of 2). Finally, the distribution of length ratios and mean distances in the set of genes where length was the discriminating factor (or where an arbitrary decision was made) shows that most of these genes were mostly identical whether measured by sequence distance or sequence length.

These results provided evidence that a sizeable fraction of recently duplicated mammalian genes are identical or very similar to each other: for roughly 30% of putative paralogs, not enough time has elapsed since the duplication event for a detectable amount of sequence change to have occurred, and the choice between retaining one copy or the other was essentially arbitrary. For the roughly 40% of putative paralogs where differences in mean distance could be identified, these differences tended to be small, suggesting that massive functional divergence of recent gene duplicates has not been a common phenomenon in mammalian evolution. Nonetheless, this protocol was designed to identify the least-diverged copy of a recently duplicated gene, and for 40% of putative paralogs the mean distance to other sequences in the gene family allowed a sensible decision to be made.

This was obviously not the most conservative approach to dealing with recent duplications—one could remove all copies from a set of putative paralogs, creating an apparent gene deletion, or one could simply ignore all gene families with any recent duplications (e.g., require one-to-one orthology allowing for gene deletions). The latter option is almost certainly too conservative, but the former option may be appropriate for a more conservative approach. As the main concern over the handling duplicated genes has been that they may introduce a bias towards elevated evolutionary rates, I marked the XYZ genes containing at least XYZ sets of putative paralogs for further evaluation. Sitewise estimates from these

genes were excluded from the most conservatively-filtered sitewise dataset and examined separately for excess signal of positive selection (see Section 1.4.2), and in the next chapter I examine whether using the more conservative approach of removing all paralogous copies from genes removed the signal of positive selection from a subset of genes (see Section ??).

1.3.4 Identifying clusters of non-synonymous substitutions

After filtering for sequence quality and removing paralogous genes and shortened gene fragments, PRANK was used to align the codon sequences of each of the 16XYZ mammalian gene trees. Manual analysis of a number of these alignments revealed many short stretches of clearly nonhomologous sequence in one species, often flanked by stretches of perfect homology and often lying on the borders of exon junctions. An example of one such region is shown in Figure ?? . In this otherwise highly conserved region of the XYZ gene, a short 20-codon stretch of the XYZ sequence appears to contain little homology to the sequences from other species.

These obviously erroneous stretches were likely due to mis-assembly of a genomic region or mis-identification of exon boundaries within the gene of one species. These errors were particularly concerning with respect to the detection of positive selection, as the incorporation of a stretch of apparently nonhomologous material into a sequence alignment would produce many alignment columns with multiple nucleotide differences per codon. As discussed in Section 1.3.1, this type of error is particularly prone to cause false positives in the detection of positive selection.

I hypothesized that these stretches of non-homologous sequence could be identified by their impact on the pattern of substitutions within each alignment. A stretch of non-homologous aligned sequence would be expected to produce a localized cluster of apparent synonymous and nonsynonymous substitutions occurring along the branch between the sequence containing the erroneous stretch and its ancestor. Because these substitutions would be restricted to one terminal branch in the gene tree and a region of the alignment limited to the length of the non-homologous stretch, a scan for clustered substitutions within the terminal lineages of genes might be an effective way of identifying these erroneous sequences.

Two factors could confound the effectiveness of using clustered substitutions to identify regions of non-homologous aligned sequence. First, the length of the terminal branch leading to each species determines how many lineage-specific substitutions would be expected to occur within a window of a certain size. The terminal human branch, for example,

is very short (as it shares a very recent common ancestor with chimpanzee), while the platypus branch is very long (sharing a most recent common ancestor only with the entire eutherian clade). Thus, one would expect to observe many more lineage-specific substitutions in platypus than in human for a given alignment window. In contrast, a stretch of non-homologous aligned sequence should introduce, on average, a constant number of non-synonymous and synonymous substitutions into the branch ancestral to the sequence in which it exists. The end result is that it should be more difficult to distinguish homologous from non-homologous stretches in species with long terminal lineages, as species with long terminal lineages will have higher numbers of substitutions in truly homologous regions. On the other hand, this trend should also serve to limit the negative impact of non-homologous stretches in those species on the detection of positive selection, because the resulting elevation in non-synonymous or synonymous substitutions rates would be less severe.

The second confounding factor is that non-synonymous substitutions have been shown to be significantly more clustered than expected by chance in a number of genomic analyses of mammalian and insect genomes [Bazykin *et al.*, 2004; Callahan *et al.*, 2011; ?]. Thus, a filter based on clustered non-synonymous substitutions may have a tendency to remove true clusters of non-synonymous substitutions from the dataset. The influence of this factor may be evaluated by comparing clusters of substitutions in terminal branches to those in internal branches: while both internal and terminal branches of the mammalian tree should harbor similar levels of truly clustered non-synonymous and synonymous substitutions, only the terminal lineages should contain large clusters resulting from stretches of aligned non-homologous sequence.

I investigated the distributions of non-synonymous and synonymous substitutions within windows of mammalian alignments by using *codeml* [Yang, 2007] under the M0 model (e.g., assuming one ω for all sites and all branches in the tree) to perform the marginal reconstruction of ancestral sequences at internal nodes [?] and to identify the substitution events implied by the reconstructed ancestral sequences of each gene alignment. Only substitution events occurring between codons with high posterior probabilities in the marginal ancestral reconstruction (> 0.9) were analyzed, and the location of each substitution event along the alignment and within the gene tree was stored. This analysis was performed on all gene trees, yielding a large database of substitution events along internal and terminal branches of the phylogenetic tree confidently inferred from the codon-based PRANK alignments of mammalian gene trees.

Using this set of inferred substitutions, counts of synonymous and non-synonymous substitutions within non-overlapping 15-codon alignment windows for all terminal and internal nodes were collected; the results for a selection of species and internal nodes are shown in Figure 1.4, which plots the number of 15-codon windows containing a given number of non-synonymous and synonymous substitutions for a selection of terminal and internal nodes. The mean length of the branch ancestral to the given node, indicated in parentheses after each node name, was calculated from the set of branch lengths estimated by *codeml*.

Figure 1.4 shows that the vast majority of 15-codon windows in these alignments contained few substitutions (note that the y-axis uses a logarithmic scale), but a long tail of non-synonymous and synonymous substitutions were observed for some nodes. Comparing the counts of non-synonymous vs. synonymous substitutions within the terminal nodes (Figure 1.4, top panel), a pattern is seen where the non-synonymous counts (red bars) are higher than synonymous counts at 0 substitutions, lower than synonymous counts in the middle range of substitutions (1–5 substitutions), and higher again in the higher range of substitutions (>5 substitutions). The pattern in the lower range is consistent with the action of purifying selection on protein-coding regions, causing a reduced number of windows with multiple non-synonymous substitutions compared to synonymous substitutions. The excess of windows with large numbers of non-synonymous substitutions, on the other hand, runs against the pattern of purifying selection; instead, it shows unexpectedly long clusters of non-synonymous substitutions to be a widespread feature of these mammalian alignments. The red and blue triangles drawn in each plot mark the number of substitutions below which 99.9% of windows are contained; the shift of the non-synonymous markers to the right emphasizes the excess of highly clustered non-synonymous substitutions. Interestingly, human—which has the highest quality and best annotated genome—does not show the same level of excess seen in the other genomes analyzed.

Comparing the pattern seen for terminal nodes to those from internal nodes provided further evidence for the presence of many stretches of non-homologous sequence within the mammalian alignments. For example, the terminal gorilla node is roughly equivalent in average branch length to the internal primates node (0.023 vs. 0.028), but gorilla contains windows with up to 14 non-synonymous substitutions while primates contain a maximum of 8. Looking at the non-synonymous and synonymous 99.9% quantiles, three of the four internal nodes had equal quantile positions for non-synonymous and synonymous substitutions, but the rodent ancestral node did not. This was an interesting difference,

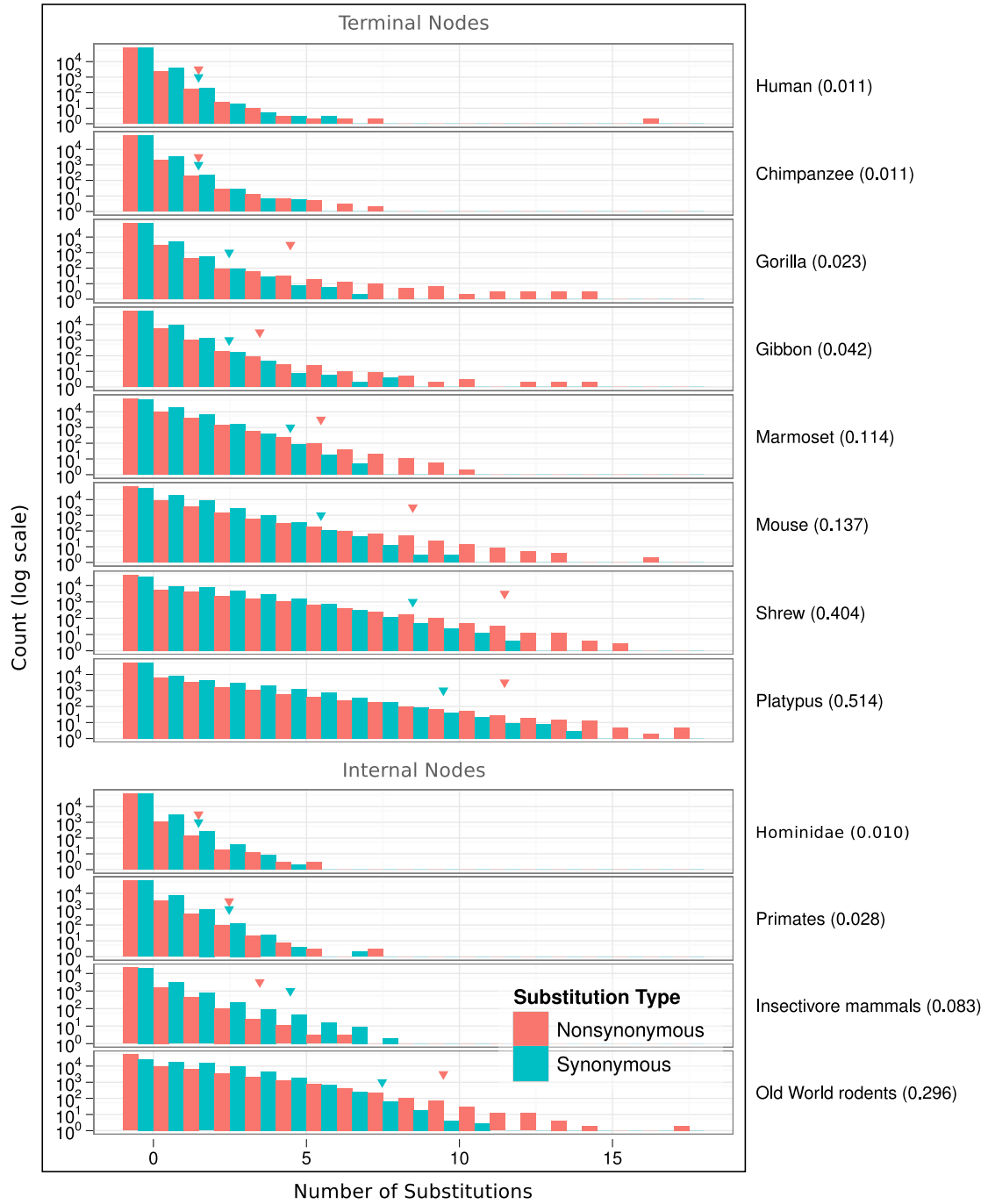


Figure 1.4: Counts of inferred non-synonymous (red bars) and synonymous (blue bars) substitutions in 15-codon windows along terminal and internal branches of the mammalian tree. The leftmost two bars correspond to windows with 0 substitutions, the next two bars correspond to windows with 1 substitution, and so on. Red and blue arrows indicate the number of non-synonymous and synonymous substitutions, respectively, corresponding to the 99.9% percentile across all windows in that node.

as the gene annotations for most rodent genomes were likely derived from alignments to mouse rather than human. In the case of discordant gene annotations, the entire rodent clade would share an aligned non-homologous stretch, causing clustered substitutions to be inferred along the internal rodent branch. This raises the possibility that the entire rodent clade contains many misaligned non-homologous stretches due to differences in gene annotations between rodent and non-rodent species. This appeared to be the case for at least one gene: Figure ?? shows the region surrounding a 15-codon window with 11 apparent rodent non-synonymous substitutions, likely the result of a difference in exon annotations between rodent and non-rodent genomes.

The end result of this analysis was the identification, for each terminal node of the mammalian tree, windows with non-synonymous substitution counts above the top 0.1% of 15-codon windows genome-wide; these windows were considered potential stretches of non-homologous aligned sequence. Despite evidence that some internal nodes might also suffer from this type of alignment artifact, most internal nodes were free from an obvious excess of clustered non-synonymous substitutions, so internal nodes were excluded from this list. And although there is no way to show that the 0.1% threshold is the most appropriate one for discriminating true from erroneous windows of clustered substitutions, manual analysis of regions containing windows at a variety of thresholds showed it to perform well.

In total, XYZ windows containing potential stretches of non-homologous aligned sequence were identified across XYZ genes, with XYZ genes containing at least 1 such window and XYZ genes containing greater than 10. The locations of these windows were stored for later use in defining the most conservatively-filtered sitewise dataset, and the impact of these potentially non-homologous windows on sitewise levels of positive selection is described in Section ??.

1.4 Genome-wide analysis of sitewise selective pressures in mammals

1.4.1 Species groups for sitewise analysis

For each alignment of mammalian orthologs, SLR was run separately on 10 different sets of mammalian species to obtain sitewise estimates in a variety of species groups. For each species group, sequences corresponding to species within the group were extracted from

Name	Count	Species List	Median dS	
			MPL	Total
Primates	10	Bushbaby, Chimpanzee, Gibbon, Gorilla, Human, Macaque, Marmoset, Mouse Lemur, Orangutan, Tarsier	0.16	0.83
Atlantogenata	5	Armadillo, Elephant, Hyrax, Sloth, Tenrec	0.26	0.97
HMRD	4	Dog, Human, Mouse, Rat	0.34	1.01
Sparse Glires	5	Guinea Pig, Kangaroo rat, Mouse, Rat, Squirrel	0.36	1.32
HQ Mammals	9	Chimpanzee, Cow, Dog, Horse, Human, Macaque, Mouse, Pig, Rat	0.31	1.61
Glires	7	Guinea Pig, Kangaroo rat, Mouse, Pika, Rabbit, Rat, Squirrel	0.40	1.90
Laurasiatheria	12	Alpaca, Cat, Cow, Dog, Dolphin, Hedgehog, Horse, Megabat, Microbat, Panda, Pig, Shrew	0.26	2.16
Sparse Mammals	7	Armadillo, Dog, Elephant, Human, Mouse, Platypus, Wallaby	0.61	2.86
Eutheria	35	Alpaca, Armadillo, Bushbaby, Cat, Chimpanzee, Cow, Dog, Dolphin, Elephant, Gibbon, Gorilla, Guinea Pig, Hedgehog, Horse, Human, Hyrax, Kangaroo rat, Macaque, Marmoset, Megabat, Microbat, Mouse, Mouse Lemur, Orangutan, Panda, Pig, Pika, Rabbit, Rat, Shrew, Sloth, Squirrel, Tarsier, Tenrec, Tree Shrew	0.35	6.43
		Alpaca, Armadillo, Bushbaby, Cat, Chimpanzee, Cow, Dog, Dolphin, Elephant, Gibbon, Gorilla, Guinea Pig, Hedgehog, Horse, Human, Hyrax, Kangaroo rat, Macaque, Marmoset, Megabat, Microbat, Mouse, Mouse Lemur, Opossum, Orangutan, Panda, Pig, Pika, Platypus, Rabbit, Rat, Shrew, Sloth, Squirrel, Tarsier, Tenrec, Tree Shrew, Wallaby	0.67	8.21
Mammals	38			

Table 1.1: Species groups used for sitewise analysis by SLR. The median MPLs and the median total branch length are shown for each species group, taken from the 15,XYZ branch lengths estimated by SLR for each gene. MPL – mean path length.

the whole mammalian alignment (along with the corresponding subtree) and input to SLR, which was run with its default parameters. If fewer than two sequences were available for a given gene and species group, the sitewise analysis was skipped for that group. The species included in each group are listed in Table 1.1 alongside the MPL and total branch length of their subtrees estimated as the median value across all 16xyz gene-wise dS branch length estimates from SLR.

Three species groups (Glires, Primates, and Laurasiatheria) were chosen because they represent the three mammalian superorders with the greatest taxonomic representation in Ensembl, providing an opportunity to compare the molecular evolutionary dynamics of three monophyletic mammalian groups containing varying levels of divergence, diverse biological characteristics, and a number of high-quality reference genomes. A fourth parallel mammalian subclade, Atlantogenata, consisting of sloth, armadillo, tenrec, elephant and hyrax, was also included, but the monophyly of this group is still under debate [Churakov *et al.*, 2009; Murphy *et al.*, 2007] and it contains only one high-coverage genome. As such, it was not considered a primary target for the mammalian superorder analysis. The different mammalian superorders contained a wide range of total branch lengths, with 0.83 for Primates, 0.97 for Atlantogenata, 1.90 for Glires, and 2.16 for Laurasiatheria.

A slightly different ordering was found when measuring the trees by MPL, with Glires having a significantly higher MPL (0.40) than the other groups despite having fewer species and a lower total branch length than Laurasiatheria. This reflected the higher neutral evolutionary rate in the Glires group, a well-documented feature of rodent evolution likely resulting from their long-term shorter generation time, which has been strongly correlated with higher neutral evolutionary rates [Nikolaev *et al.*, 2007; Smith & Donoghue, 2008].

Two larger species groups, Eutheria and Mammalia, were chosen for the purpose of measuring average sitewise selective pressures across mammals as a whole. The Eutheria group consists of the union of the mammalian superorder groups plus armadillo, and the Mammalian group adds opossum, platypus, and wallaby for a total of 38 species. The median total branch lengths for Mammalia and Eutheria were 8.21 and 6.43, respectively, and the MPLs were 0.67 and 0.35.

Finally, to evaluate the impact of species choice and branch length on the results of the sitewise analysis, four additional “sparse” species groups were created for comparison to the main groups of interest. The species in the Sparse Glires group were chosen to create a group with species from the Glires group but having a lower overall branch length; the Sparse Mammals group was created with a similar aim, created by selecting one species (preferably with a high-coverage genome) from each major mammalian branch, greatly reducing the total branch length covered but maintaining a similar evolutionary depth and distribution of major branches within the species tree. The HQ Mammals group was similar to the Sparse Mammals group, but elephant and the deeper mammalian lineages were omitted (e.g., wallaby, platypus, armadillo) in favor of only the high-coverage Eutherian genomes (e.g., chimpanzee, cow, horse, macaque, pig, rat). Finally, the HMRD group consisted of human, mouse, rat, dog, and represented the type of phylogenetic tree that was commonly analyzed early in the last decade when only a few mammalian genome sequences were available. The HMRD group was comparable to Primates and Atlantogenata in total branch length, while HQ Mammals and Sparse Glires were more similar to Glires.

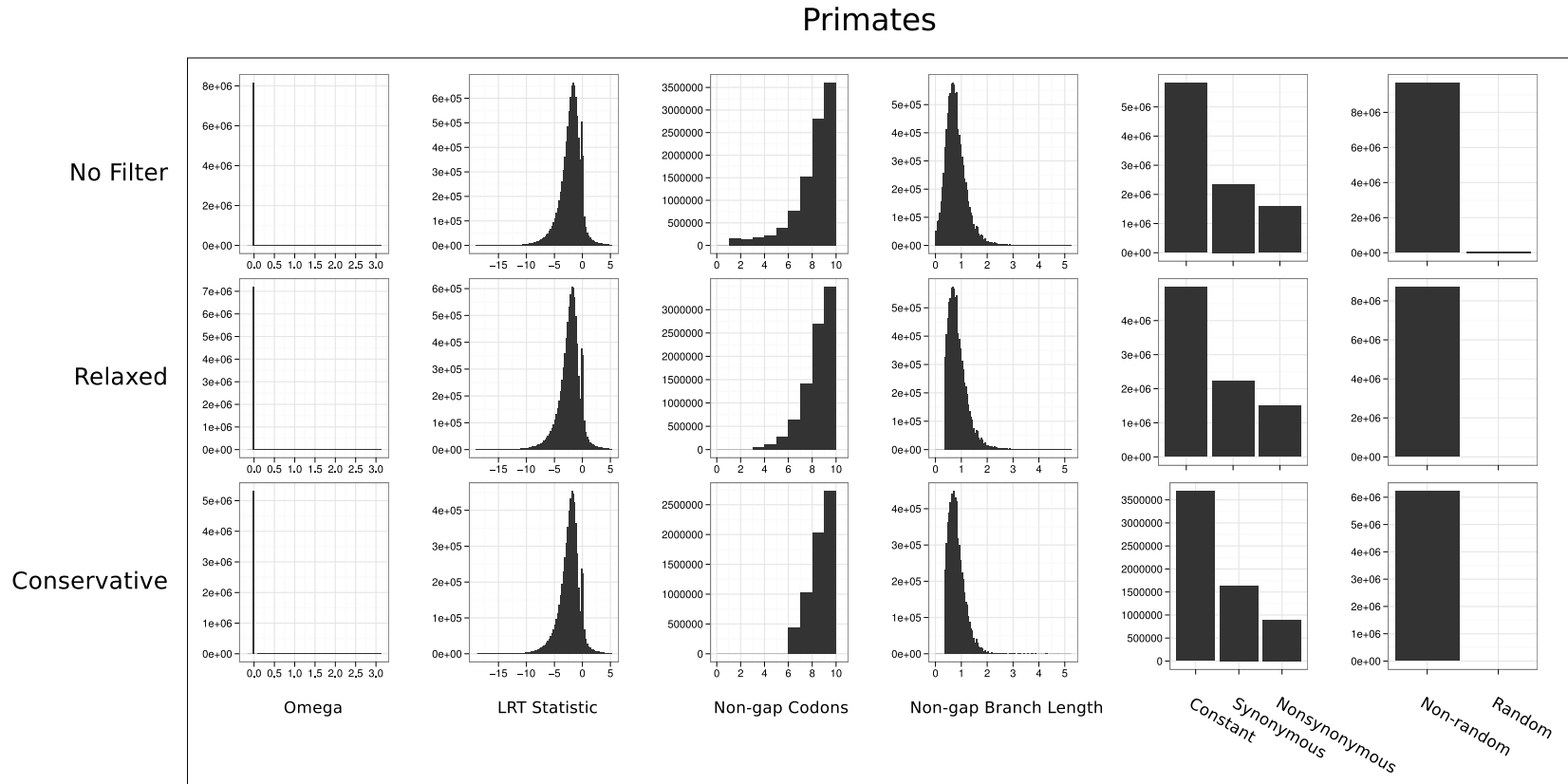


Figure 1.5: Distributions of sitewise values for the Primates species group, showing the raw data (top row) and the result of applying the relaxed (middle row) and conservative (bottom row) filters.

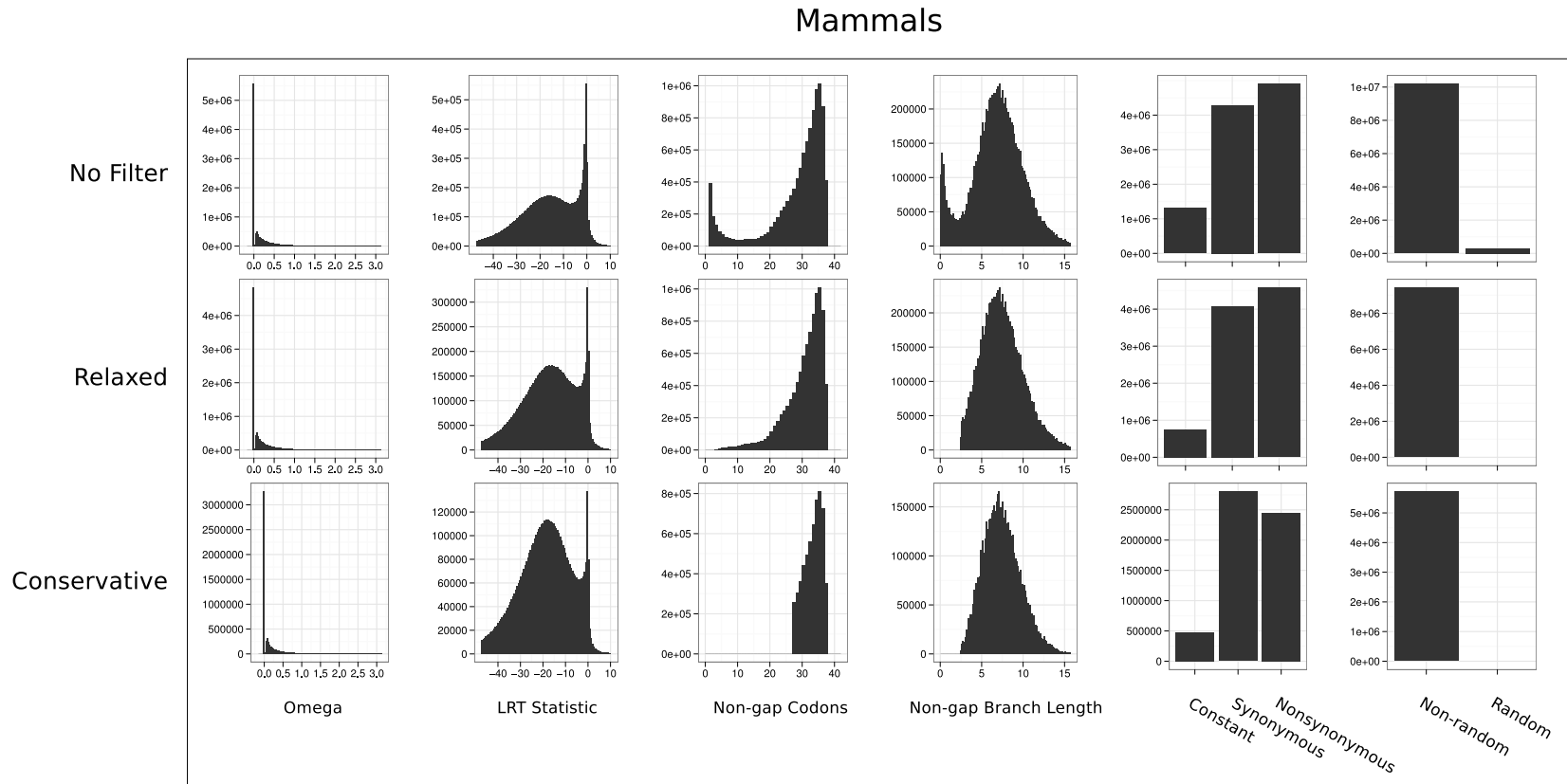


Figure 1.6: Distributions of sitewise values for the Mammals species group, showing the raw data (top row) and the result of applying the relaxed (middle row) and conservative (bottom row) filters.

1.4.2 Evaluation of the bulk distributions and the design of a filtering approach

Sitewise data were collected from SLR and stored in a database for storage and further analysis. The Mammals group, containing the most branch length of all the datasets and representing the entire set of aligned sequences, and the Primates group, containing the lowest overall branch length, were used as representative species groups to perform quality-control checks on the sitewise data and to guide the curation of filtered sitewise datasets for each species group.

Some amount of filtering is usually necessary in genomic analyses, and the situation is especially delicate in a scan for positive selection, since non-biological artifacts often appear to represent elevated evolutionary rates [Mallick *et al.*, 2009; Markova-Raina & Petrov, 2011; Schneider *et al.*, 2009]. To balance the desire to maintain as much real data as possible with the concern that a methodological bias may influence the results, two datasets were generated by processing sitewise data separately with two filters: a relaxed filter, designed to retain much of the data while filtering out the most obviously low-quality sites, and a conservative filter, designed to remove a wider set of sites and genes that showed evidence for potential errors or biases.

I first examined the overall distributions of ω estimates and sitewise LRT statistics from SLR. Figures 1.5 and 1.6 show the distributions of six sitewise values for each group of species: two continuous values and two categorical values output by SLR (Omega, Signed LRT, Site Pattern and Random) and two values calculated from the codon alignment (Non-gap Codons and Non-gap Branch Length). Non-gap Codons is a count of the number of non-gap codons in each alignment column, and the Non-gap Branch Length value represents the total branch length connecting all non-gap sequences (using the gene-wide branch lengths optimized by SLR).

A prominent feature of the distribution of ω values for the unfiltered Mammals data, shown in the top row of Figure 1.6, was the large number of sites with a zero value for ω_{ML} , the maximum likelihood (ML) point estimate of ω . Further inspection of the data revealed that all $\omega_{ML} = 0$ sites contained either synonymous or constant site patterns. Furthermore, all sites with constant patterns (and nearly all sites with synonymous patterns) yielded a ω_{ML} estimate of zero. Intuitively, an estimate of zero for synonymous sites is appropriate, as the lack of any non-synonymous substitutions throughout the tree would provide no evidence for a non-synonymous substitution rate of greater than zero. For constant sites the case is less clear, because no data regarding the rate of either syn-

onymous or non-synonymous substitutions exists in the alignment column. However, given SLR’s assumption of a constant synonymous substitution rate throughout each gene [Massingham & Goldman, 2005], the ω value which maximizes the likelihood of observing zero substitutions is zero, since that value minimizes both the non-synonymous and the total substitution rate.

It is not evident from Figure 1.6, but a small proportion (ca. 0.2%) of sites containing synonymous site patterns resulted in maximum likelihood estimates greater than zero. Analysis of the alignment columns corresponding to these sites showed them all to include synonymous codons coding for serine or arginine which are separated by multiple nucleotide differences. Under the mechanistic codon model implemented by SLR, which does not allow for multiple simultaneous nucleotide changes, inferring an evolutionary path between these multiply-substituted codons required the inference of multiple non-synonymous substitutions to reach one codon from the other. This produced a non-synonymous substitution rate of greater than zero for a site with a synonymous site pattern. The existence of multiply-substituted codons in alignments has been previously reported [Averof *et al.*, 2000; Whelan & Goldman, 2004], and empirical results have supported the notion that codon models that allow for multiple simultaneous nucleotide changes better describe evolution than those that do not [Kosiol *et al.*, 2007]. However, the very low proportion of synonymous sites requiring nonzero non-synonymous substitution rates suggested that the impact of these effects on the current dataset was minimal; this is likely due to the relatively short branch lengths separating the nodes of the mammalian tree, making it less probable that codons with multiple substitutions (whether the result of simultaneous multiple nucleotide changes or successive single changes) would be observed [Kosiol *et al.*, 2007].

The distributions of the Non-gap Codons and Non-gap Branch Length values in the unfiltered row of Figure 1.6 showed that most alignment columns contained sequence data from many species (with Non-gap Codons peaking at 36 and Non-gap Branch Length peaking at around 8 substitutions per site), but a noticeable portion contained only a few non-gap sequences. If the alignment columns with low non-gap codon counts represented accurate evolutionary histories, then the observed excess of highly-gapped sites might be taken as an indication that insertion events in terminal lineages or recent ancestral lineages were prominent enough throughout mammalian evolution to leave a noticeable signature of sites with very low non-gap codon counts. Given the many possible sources of error in the annotation and alignment of these sequences, however, a more likely scenario was that

	BL	Nongap BL			Nongap Codons			ω_{ML} , %		PSC _{5%} , %
	Quantile	25%	50%	75%	25%	50%	75%	< 1	> 1	
Mammals	0.10	0.31	0.74	1.46	2	3	6	81.87	18.13	2.09
	0.20	3.28	3.78	4.17	19	30	35	95.01	4.99	0.52
	0.30	4.77	5.02	5.24	27	33	36	96.90	3.10	0.35
	0.40	5.67	5.86	6.04	28	33	36	96.94	3.06	0.35
	0.50	6.38	6.55	6.72	29	33	36	96.75	3.24	0.39
	0.60	7.06	7.22	7.40	29	33	36	96.41	3.59	0.44
	0.70	7.77	7.95	8.15	29	33	36	96.04	3.96	0.50
	0.80	8.58	8.79	9.03	29	33	35	95.43	4.57	0.61
	0.90	9.58	9.88	10.24	29	33	35	94.57	5.43	0.79
	1.00	11.22	12.00	13.28	29	32	35	92.95	7.04	1.14
Primates	0.10	0.17	0.25	0.30	4	6	8	94.42	5.58	0.61
	0.20	0.38	0.41	0.44	8	9	10	94.39	5.61	0.32
	0.30	0.49	0.52	0.54	8	9	10	93.64	6.36	0.30
	0.40	0.59	0.61	0.63	8	9	10	93.09	6.91	0.33
	0.50	0.67	0.69	0.71	8	9	10	92.39	7.61	0.35
	0.60	0.76	0.78	0.80	8	9	10	91.29	8.71	0.46
	0.70	0.85	0.87	0.90	8	9	10	90.68	9.32	0.50
	0.80	0.97	1.00	1.04	8	9	10	89.10	10.90	0.66
	0.90	1.13	1.19	1.25	9	9	10	87.13	12.87	0.86
	1.00	1.44	1.61	1.95	8	9	10	84.64	15.36	1.24

Table 1.2: Proportions of sites with evidence for purifying and positive selection in the Mammalia and Primates datasets broken down by non-gap branch length. Sites were separated into 10 equally-sized bins of non-gap branch length and the sites within each bin were summarized by the 25th, 50th and 75th percentiles of non-gap branch length (BL) and non-gap codons, the percentage of sites with ω estimated below or above 1, and the percentage of sites classified as positively-selected codons (PSCs) at a nominal 5% FPR. BL—branch length; PSC—positively selected codons.

sites with low codon counts and low branch lengths came from stretches of sequence which only exist in a few species as a result of annotation or alignment error. As a result, these sites might be expected to show a higher probability of being nonhomologous and showing spurious signals of positive selection. This would make such sites prime candidates for filtering out prior to analysis.

To test the hypothesis that sites with few non-gap sequences would be less reliable for analysis than other sites, I split the sitewise estimates from the Mammals and Primates groups into ten equally-sized bins of non-gap branch length. Sites within each bin were summarized by calculating the percentage of sites with ω_{ML} less than or greater than 1, as well as the percentage of sites showing evidence for positive selection at a nominal 5% false positive rate (FPR), hereafter referred to as positively selected codons (PSCs).

The results of this analysis are presented in Table 1.2. The lowest bin was a clear outlier in the Mammals data, with nearly 17% of sites having $\omega_{ML} > 1$ and 2% of sites being PSCs. The other 9 bins with greater non-gap branch lengths showed fewer sites with $\omega > 1$ and less evidence for positive selection; within those 9 bins, a pattern of gradual increase in the proportion of sites with $\omega_{ML} > 1$ and PSCs was observed at progressively higher non-gap branch lengths. The increase in evidence for positive selection with increasing non-gap branch length could be explained by genes with higher overall dN/dS ratios (and presumably more PSCs) having higher branch lengths due to the increased rate of non-synonymous substitution. Overall, the pattern observed for the Mammals data was consistent with the prediction that sites with few non-gap sequences were not consistent with the general pattern of sitewise data. In terms of choosing an appropriate threshold on which to filter, Table 1.2 indicated that removing sites with the lowest 10% of non-gap branch length would remove most of the apparently anomalous sites.

Table 1.2 showed a similar trend for the Primates dataset, although the distinction between the lowest bin and the rest of the dataset was less obvious. The percentage of PSCs in the lowest decile was only slightly higher than in the next-highest decile, and the proportion of sites with $\omega_{ML} > 1$ was lower than in all other bins. Thus, despite weaker evidence in the Primates data for the anomalous nature of sites with few non-gap sequences, it still appeared that filtering sites in the bottom 10% bin would improve the overall quality and consistency of the data.

Turning back to the bulk distributions in Figure ??, two other criteria were used to target sites for removal before analysis. First, the rightmost panels of Figures 1.6 and 1.5 depict a small set of sites designated as “random”. These sites were flagged by SLR as having a site pattern not significantly different from random [Massingham & Goldman, 2005], and they were also targeted for removal before analysis of the global distribution. Second, all sites with fewer than four non-gap sequences were removed. This was done to avoid analyzing sites with very few sequences which were not within the bottom 10% of sites by non-gap branchlength.

At this point, all of the criteria used to define the relaxed filter have been described: non-gap branch lengths, random flags, and the number of non-gap sequences at each site. The middle rows of Figures 1.5 and 1.6 show the summary distributions resulting from applying the relaxed filter to the Mammals and Primates sitewise data.

Three additional criteria were added to create the more conservative filtered dataset. First, the threshold on non-gap sequence counts was increased: all sites with a non-gap

codon count below 75% of the maximum non-gap count for that species group were removed. Second, sites and genes containing windows of clustered non-synonymous substitutions (as identified in Section 1.3.4) were removed: all sites overlapping the 23,116 15-codon windows with excess non-synonymous substitutions (using the 99.9% quantile based definition of excess substitutions from Section 1.3.4) were masked out, and 819 genes with greater than 10% of sites covered by windows with excess non-synonymous substitutions were removed. Finally, the 3,333 genes which contained more than 2 sets of putative paralogs were excluded.

As with the relaxed filter the result of applying the conservative filter to the Primates and Mammals datasets is shown in the bottom rows of Figures 1.5 and 1.6. Comparing between the distributions in the three rows of Figure 1.6, the most prominent effect of the two filters on the bulk distributions in was the removal of the excess of sites with low non-gap branch lengths and non-gap codon counts. The distributions of ω_{ML} estimates and LRT statistics were qualitatively unchanged, indicating that the overall characteristics of the dataset were not significantly altered by this filter.

Tables 1.3 and 1.4 provide a quantitative summary of the Mammals and Primates datasets before and after applying the two filters. Also shown is the subset of sites overlapping with Pfam domain annotations collected from Ensembl; as most Pfam domains represent well-folded protein modules [Finn *et al.*, 2010], the set of Pfam-annotated sites were expected to exhibit stronger purifying selection and be less prone to insertions or deletions and alignment error. The rows labeled in parentheses summarize the set of sites which were removed during the creation of the conservatively-filtered dataset, either due to overlap with a window of clustered substitutions (Clusters) or from being within a gene that contained more than 2 recent duplications (Paralogs).

The impact of extensive filtering on the genome-wide levels of positive and purifying selection becomes clear in this view. The unfiltered data from the Primates group contained 9.07% of sites with $\omega_{ML} > 1$, and 0.59% of sites were PSCs at a nominal 5% FPR; the evidence for positive selection was reduced in the conservatively-filtered data, showing 7.87% sites with $\omega_{ML} > 1$ and 0.41% PSCs. An even stronger effect of filtering was seen for the Mammals data, with $\omega_{ML} > 1.5$ being reduced from 5.71 to 2.73 between the unfiltered and conservatively-filtered datasets, and the percentage of PSCs reduced from 0.72% to 0.35%. The rows representing two sets of sites which were removed during the conservative filtering process showed higher signals of positive selection than the unfiltered data, suggesting that these two filtering steps were at least somewhat effective in removing

potentially anomalous or untrustworthy sites from the dataset.

Name	Filter	Sites	Site Pattern, %			Med. Codons	Nongap BL			ω_{ML}		ω_{ML} Below / Above, %			
			Const.	Syn.	Nsyn.		Med.	Mean	SD	Mean	SD	< 0.5	< 1	> 1	> 1.5
Primates	None	9.76e+06	59.69	24.07	16.24	9	0.74	0.86	1.22	0.23	0.63	85.97	90.93	9.07	5.88
	Relaxed	8.71e+06	57.24	25.51	17.25	9	0.79	0.94	1.27	0.23	0.62	85.22	90.73	9.27	5.79
	Conservative	6.22e+06	59.29	26.26	14.45	9	0.76	0.82	0.50	0.19	0.57	87.27	92.13	7.87	4.80
	Pfam	2.33e+06	58.98	27.47	13.55	9	0.77	0.94	1.72	0.17	0.52	88.91	93.52	6.48	3.87
	(Clusters)	9.74e+05	44.25	21.59	34.17	9	1.18	1.44	1.45	0.46	0.83	71.66	81.72	18.28	11.99
	(Paralogs)	1.64e+06	52.37	25.13	22.50	9	0.87	1.33	2.65	0.27	0.66	82.58	89.26	10.74	6.73
Mammals	None	1.05e+07	12.43	40.80	46.77	32	6.95	6.95	4.15	0.22	0.47	86.20	94.29	5.71	2.94
	Relaxed	9.42e+06	8.03	43.36	48.61	33	7.30	7.63	3.82	0.19	0.37	87.49	95.75	4.25	1.62
	Conservative	5.72e+06	8.30	48.98	42.72	34	7.28	7.48	2.42	0.15	0.30	90.86	97.27	2.73	0.91
	Pfam	2.48e+06	8.68	50.49	40.83	33	7.28	7.66	4.81	0.13	0.30	91.94	97.49	2.51	0.92
	(Clusters)	9.92e+05	4.33	22.06	73.61	29	9.50	9.68	4.86	0.40	0.52	71.95	88.84	11.15	4.69
	(Paralogs)	1.82e+06	7.18	38.51	54.31	31	7.70	8.33	6.84	0.22	0.40	85.29	94.84	5.16	2.03

Table 1.3: Summary statistics of sitewise estimates for Mammals and Primates data with various filters applied. Rows labeled (Clusters) and (Paralogs) contain sites excluded by the Conservative filter. Columns under the “ ω_{ML} Below / Above” heading measure the percentage of sites with ω_{ML} below or above the indicated value. Med.—median, Const.—constant, Syn.—synonymous, Nsyn.—non-synonymous, BL—branch length.

Name	Filter	Positively Selected Sites (%)								$P_{\chi_1^2} < 0.1$, %			$P_{\chi_1^2} < 0.05$, %		
		$P_{\chi_1^2} < 0.1$		$P_{\chi_1^2} < 0.05$		$P_{\chi_1^2} < 0.01$		FDR < 0.05		Neg.	Neut.	Pos.	Neg.	Neut.	Pos.
Primates	None	99002	(1.01)	57919	(0.59)	18277	(0.19)	243	(0.002)	29.93	69.05	1.01	14.31	85.09	0.59
	Relaxed	82607	(0.95)	47825	(0.55)	14619	(0.17)	104	(0.001)	33.27	65.79	0.95	15.98	83.47	0.55
	Conservative	45179	(0.73)	25710	(0.41)	7661	(0.12)	50	(0.001)	33.89	65.38	0.73	15.88	83.70	0.41
	Pfam	13988	(0.60)	8050	(0.35)	2440	(0.10)	23	(0.001)	37.73	61.67	0.60	18.80	80.85	0.35
	(Clusters)	23808	(2.44)	14331	(1.47)	4707	(0.48)	40	(0.004)	30.73	66.82	2.44	16.61	81.92	1.47
	(Paralogs)	19175	(1.17)	11269	(0.69)	3496	(0.21)	30	(0.002)	33.87	64.96	1.17	17.72	81.59	0.69
Mammals	None	114094	(1.09)	75509	(0.72)	30692	(0.29)	2052	(0.020)	80.21	18.71	1.09	77.03	22.25	0.72
	Relaxed	76370	(0.81)	52096	(0.55)	23323	(0.25)	1879	(0.020)	86.51	12.68	0.81	83.88	15.57	0.55
	Conservative	29075	(0.51)	19900	(0.35)	9025	(0.16)	781	(0.014)	90.61	8.88	0.51	88.54	11.11	0.35
	Pfam	12756	(0.51)	8956	(0.36)	4353	(0.18)	428	(0.017)	91.58	7.91	0.51	89.70	9.93	0.36
	(Clusters)	23716	(2.39)	16531	(1.67)	7648	(0.77)	659	(0.066)	70.07	27.54	2.39	65.66	32.67	1.67
	(Paralogs)	18090	(0.99)	12394	(0.68)	5551	(0.30)	432	(0.024)	83.83	15.18	0.99	80.76	18.56	0.68

Table 1.4: Proportions of sites subject to positive, purifying and neutral selection at various LRT_{SLR} thresholds for Mammals and Primates data with various filters applied. The Benjamini-Hochberg method [Benjamini & Hochberg, 1995] was used to identify the LRT_{SLR} threshold at which $FDR < 0.05$. For columns under the headings “ $P_{\chi_1^2} < 0.1$, %” and “ $P_{\chi_1^2} < 0.05$, %”, Pos. and Neg. are the percentage of sites with significant evidence for positive and negative selection, respectively, and Neut. is the percentage of “neutral” sites not showing significant evidence for non-neutral selection.

1.4.3 The global distribution of sitewise selective pressures in mammals

The sitewise data from each of the ten species groups were processed with the conservative filter as described above. The resulting global distributions of site patterns, sitewise ω_{ML} estimates, and 95% confidence intervals are shown in Figure 1.7. The left panel in each row plots the number of sites with constant, synonymous, and non-synonymous patterns; all sites with $\omega_{ML} = 0$ had constant or synonymous patterns, and all sites with $\omega_{ML} > 0$ had non-synonymous patterns. The right panel in each row shows the distributions of ω_{ML} for sites which contained a non-synonymous site pattern.

1.4.3.1 Site patterns and ω_{ML} values reveal the prevalence of purifying selection in mammalian proteins

The site pattern counts in Figure 1.7 showed that the branch length of each species group had a strong effect on the overall composition of the sitewise data. Species groups covering little branch length, such as Primates and Atlantogenata, contained mostly constant sites, while groups covering a large amount of branch length, such as Eutheria and Mammals, contained few constant sites and roughly equal proportions of sites with synonymous and non-synonymous site patterns. Comparing the Glires and Mammals data with their corresponding “sparse” datasets confirmed that this trend was largely due to branch length as opposed to biological factors: the Sparse Glires data, for example, yielded a smaller proportion of non-synonymous sites and a greater proportion of constant sites than the Glires data (17.41% versus 24.08% for non-synonymous sites, 44.21% versus 33.98% for constant sites).

The distributions of ω_{ML} estimates are shown in Figure ?? as a series of histograms showing the ω_{ML} density (for nonzero values of ω_{ML} only) and a series of solid lines showing the cumulative ω_{ML} density (representing all values); the lower and upper dashed lines show the cumulative density of the lower and upper 95% confidence interval resulting from each sitewise estimate. From these distributions, it is clear that the majority of protein-coding sites have evolved under purifying selection in mammals, a fact which is most easily seen in the larger species groups. The Mammalia group, which contained only a small proportion of uninformative constant sites (8.17%), showed a maximum density of nonzero ω_{ML} estimates at $\omega \approx 0.1$, and the vast majority of sites showed some evidence of purifying selection with ω_{ML} estimates below 1. The height of the ω_{ML} cumulative distribution at

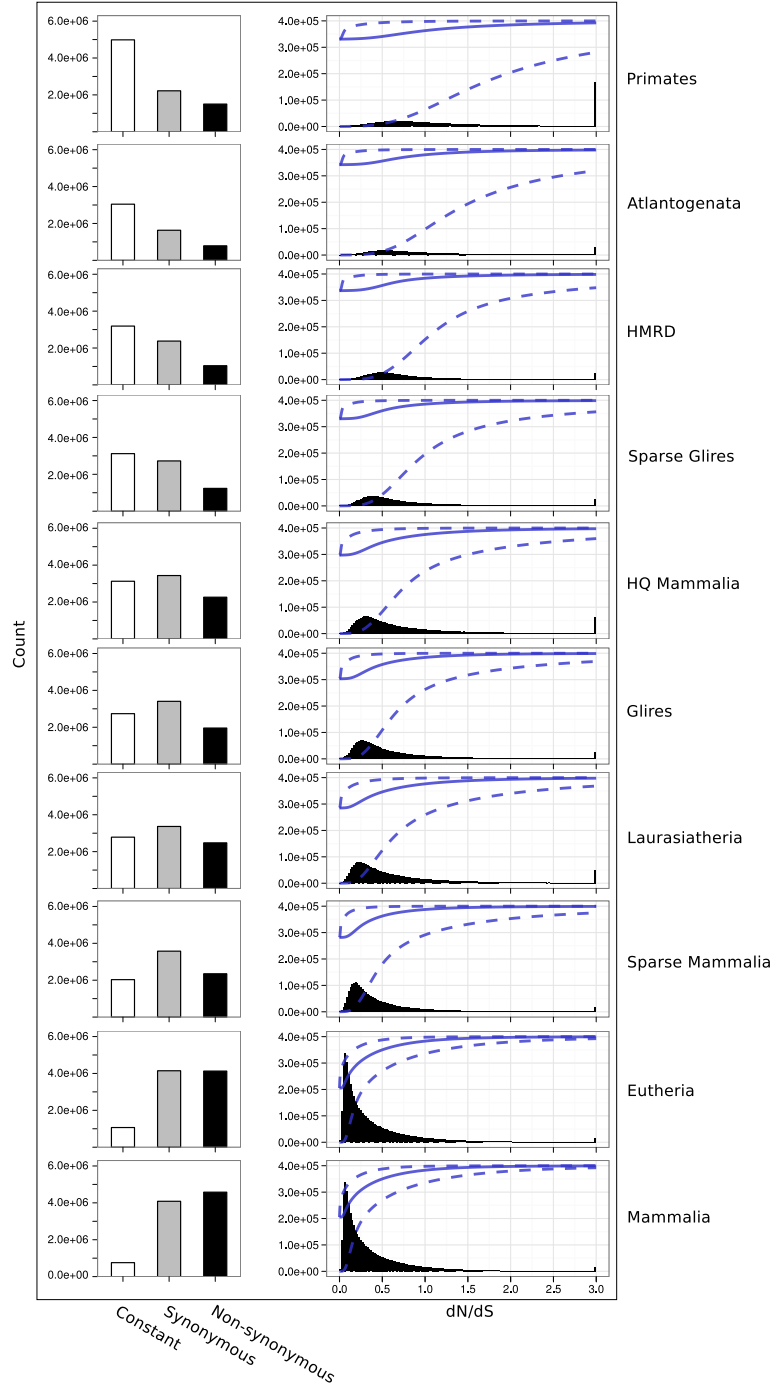


Figure 1.7: Global distributions of site patterns and ω estimates for ten species groups. Left panels: bars represent the number of sites showing constant, synonymous, and non-synonymous patterns. Note, the y-axis is held constant between rows. Right panels: bars represent histograms of ω_{ML} estimates for sites where $\omega_{ML} > 0$. Sites with $\omega_{ML} > 3$ are counted in the bin at $\omega_{ML} = 3$. A solid line is drawn showing the cumulative distribution of ω_{ML} , and dashed lines are drawn above and below the solid line showing the cumulative distributions of the lower and upper bounds, respectively, of the 95% confidence interval associated with each sitewise estimate.

$\omega = 1$ corresponds to the proportion of sites with some evidence for purifying selection. The nonzero ω_{ML} values were more evenly spread in the other species groups: Glires contained a maximum nonzero ω_{ML} density at around $\omega \approx 0.25$ and Primates at $\omega \approx 0.7$. This upwards shift in nonzero ω_{ML} estimates relative to Mammalia was likely due to the greater proportion of constant and synonymous sites in datasets with lower overall branch lengths: sites which were truly evolving with $0 < \omega < 1$, but where no non-synonymous or synonymous substitutions were observed, would have their ω_{ML} estimate “pushed” towards zero, presumably causing a concomitant upwards shift in the distribution of the remaining nonzero ω_{ML} values.

1.4.3.2 Sitewise confidence intervals and LRT statistics identify sites with significant evidence for purifying and positive selection

An important component of SLR’s output is the set of statistics providing information about the confidence with which purifying or positive selection was detected. These values include the lower and upper bounds of $CI_{95\%}$, the 95% confidence interval for each ω_{ML} estimate, and the LRT statistic, which corresponds to the strength of evidence for purifying or positive selection. Following Massingham [2005], I used a signed version of the LRT statistic (hereafter LRT_{SLR}), formed by negating the LRT statistic for sites where $\omega_{ML} < 1$, as a way to sort sites according to their evidence for purifying and positive selection. Thus, sites with $LRT_{SLR} < 0$ showed at least some evidence for purifying selection, and sites with $LRT_{SLR} > 0$ showed at least some evidence for positive selection. It should be noted that the LRT_{SLR} is a measure of the strength of evidence for purifying or positive selection, but not necessarily the actual strength of that selection. For example, an alignment covering a very large branch length might yield a strongly negative LRT_{SLR} for a site with ω_{ML} only moderately below 1, because the evidence for purifying selection at that site was highly statistically significant; on the other hand, a strongly-purifying site in an alignment covering less branch length might produce a much less-negative LRT_{SLR} , even with an estimated ω_{ML} near zero.

To further explore this point, Figure 1.8A shows the relationship between LRT_{SLR} , ω_{ML} and the $CI_{95\%}$ width for sites from the Mammals group. The left panel, comparing the LRT_{SLR} to nonzero ω_{ML} estimates, shows that the two values are highly correlated, with the greatest number of low ω_{ML} estimates occurring at sites with strongly negative LRT_{SLR} s. Correspondingly, the middle panel shows an even stronger relationship between the LRT_{SLR} magnitude and the $CI_{95\%}$ width, with the tightest confidence intervals at

sites with very strong evidence for purifying selection. The rightmost panel compares the ω_{ML} of each site with the width of its $CI_{95\%}$, revealing a more linear and diffuse positive relationship between ω_{ML} and the size of the $CI_{95\%}$. The equivalent plots for Primates, shown in Figure 1.8B, reveal similar patterns, but with generally less-negative LRT_{SLR} values, higher ω_{ML} , and larger $CI_{95\%}$. These differences highlight the impact of branch length on the amount of confidence with which ω can be estimated on a per-site basis. The low branch length of the Primates clade rarely yields ω_{ML} estimates with $CI_{95\%}$ intervals smaller than 1, while the bulk of sites from the Mammalia dataset have relatively small $CI_{95\%}$ s. Thus, the distribution of ω_{ML} estimates from datasets with low branch lengths (e.g., the histogram densities seen in Figure 1.7) should be interpreted with caution, as any comparison between ω_{ML} from different sites or datasets may be more sensitive to the amount of statistical confidence placed on each estimate than to any meaningful biological difference between the two sets of data.

Instead, the statistical information at each site could be used to identify sites evolving under purifying or positive selection with confidence. Sites with CI_{upper} , the upper bound of the $CI_{95\%}$ interval, below $\omega = 1$ can be interpreted as having evidence of purifying selection with an expected 5% FPR; likewise, sites with CI_{lower} above $\omega = 1$ contain evidence of positive selection with an expected 5% FPR. In both cases, the 5% FPR is the level expected under SLR's null model of neutral evolution. There was a strong relationship between CI_{upper} and the χ^2_1 approximation to the LRT_{SLR} distribution, whereby the set of sites with $CI_{upper} < 1$ was exactly equivalent to the set of sites with LRT_{SLR} below the negative χ^2_1 95% critical value. Similarly, the sites with $CI_{lower} > 1$ were those with LRT_{SLR} above the χ^2_1 95% critical value. Because of this equality, I will generally refer to LRT_{SLR} values instead of $CI_{95\%}$ intervals when discussing sites with significant evidence for purifying or positive selection.

Table 1.6, which shows the same values included in Table 1.4 for different filtering groups, summarizes the results from using the χ^2_1 approximation to the LRT_{SLR} distribution to identify sites subject to purifying selection and positive selection at various FPR thresholds. The left group of columns show the number and proportion of sites with evidence for positive selection at nominal 10%, 5%, and 1% FPR thresholds, respectively, as well as an expected 5% FDR calculated using the Benjamini Hochberg method for FDR control [Benjamini & Hochberg, 1995]. The two groups of columns on the right show the result of breaking sites into three groups (positive, negative, and neutral) based on the result of a χ^2_1 test at a given FPR threshold.

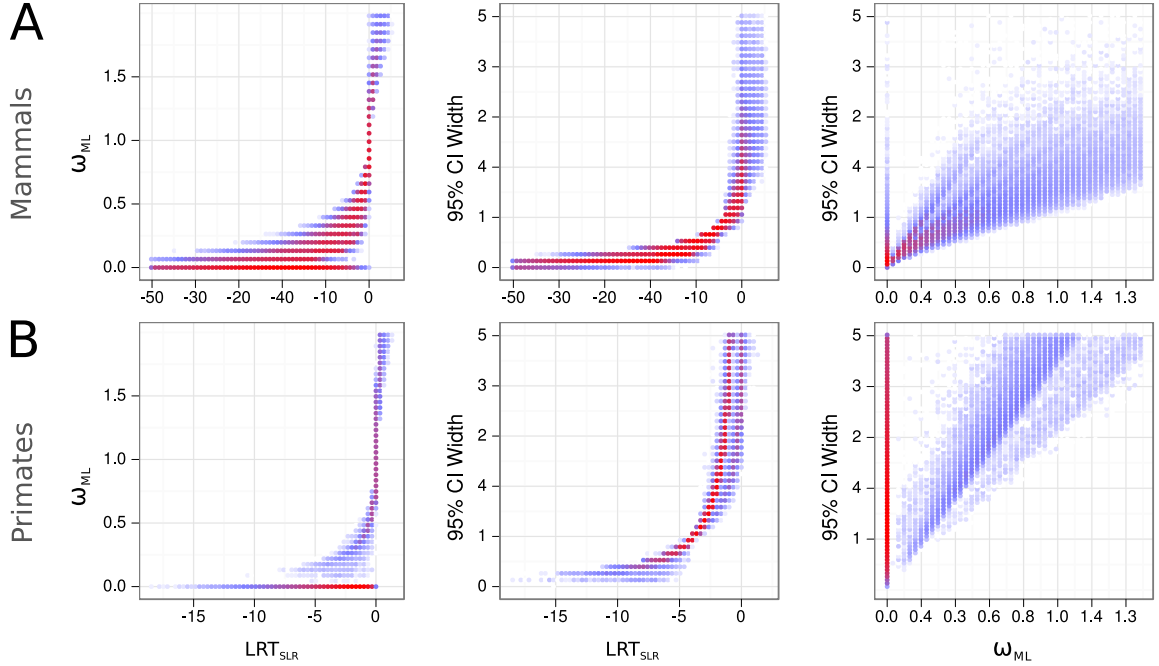


Figure 1.8: The relationship between LRT_{SLR} , ω_{ML} , and $CI_{95\%}$ width in (A) Mammalia and (B) Primates datasets. Each point represents the binned density of sites; no points are drawn where no density exists, while blue and red points are drawn at areas of low and high density, respectively. The left panel shows sites where $\omega_{ML} < 0$, the middle panel shows all sites, and the right panel shows sites where $0 < \omega_{ML} < 1$. Note the change in x-axis scales between plots in (A) and (B), reflecting the paucity of sites in Primates with strong evidence ($LRT_{SLR} < -12$) for purifying selection.

The positive selection results demonstrated that anywhere between 0.01% to 0.73% of sites could be confidently identified as under positive selection in mammals at nominal FPR thresholds between 1% and 10%, but different species groups yielded strikingly different estimates of the proportion of PSCs. At a 5% FPR threshold, the Primates, HQ Mammals, Laurasiatheria, Eutheria, and Mammals groups produced broadly comparable proportions of positively-selected sites, ranging from 0.33% to 0.42%. The proportions of PSCs in these groups were higher using a 10% FPR threshold (ranging from 0.46% to 0.73% of sites) and lower using a 1% FPR threshold (ranging from 0.07% to 0.19%). When the FDR was controlled using the Benjamini-Hochberg method, however, far fewer PSCs were identified. Only the Eutheria and Mammalia groups yielded a substantial number of positively-selected sites at this level of control; the Primates and Laurasiatheria

data yielded a small number of PSCs, but these species groups were likely limited in their power to yield positively-selected sites after FDR control due to their lower total branch lengths. Interestingly, the Atlantogenata, HMRD, Sparse Glires, Glires and Sparse Mammalia datasets all produced much lower proportions of positively-selected sites across all FPR thresholds. At $FDR < 0.05$, all four groups yielded zero significant PSCs, and at a 1% FPR they all contained lower than 0.01% PSCs.

In Mammalia, the breakdown of sites into positive, negative and neutral categories at 10% and 5% significance thresholds produced a pattern similar to that seen in the ω_{ML} distribution, with a large amount of purifying constraint (83.87% of sites at 5% FPR), a small proportion of neutrally-evolving sites (15.57%), and a diminishing number of positively-selected sites (0.55%). As expected given the use of a fixed LRT_{SLR} threshold to identify purifying sites, the fraction of sites confidently identified as under purifying selection showed a strong dependency on the branch length of the species set, with a much higher power in Mammalia than in Primates to confidently detect purifying selection (83.87% vs. 15.97%).

Name	Filter	Sites	Site Pattern, %			Med. Codons	Nongap BL			ω_{ML}		ω_{ML} Below / Above, %			
			Const.	Syn.	Nsyn.		Med.	Mean	SD	Mean	SD	< 0.5	< 1	> 1	> 1.5
Primates	Conservative	6.22e+06	59.29	26.26	14.45	9	0.76	0.82	0.50	0.19	0.57	87.27	92.13	7.87	4.80
Atlantogenata		4.07e+06	57.23	30.07	12.70	5	0.94	1.01	0.37	0.13	0.41	90.01	95.38	4.62	2.29
HMRD		5.02e+06	49.75	36.41	13.84	4	0.96	1.01	0.36	0.12	0.37	90.06	96.37	3.63	1.73
Sparse Glires		5.35e+06	45.36	39.11	15.53	5	1.24	1.32	0.68	0.12	0.36	90.91	96.71	3.29	1.51
HQ Mammals		6.38e+06	37.09	40.68	22.23	8	1.46	1.55	0.64	0.17	0.43	88.31	94.97	5.03	2.50
Glires		5.79e+06	34.70	43.68	21.62	7	1.77	1.87	0.84	0.13	0.36	90.54	96.53	3.47	1.50
Laurasiatheria		5.35e+06	33.36	41.99	24.66	11	2.03	2.15	0.87	0.16	0.41	88.88	95.36	4.64	2.22
Sparse Mammals		5.65e+06	25.81	46.75	27.44	6	2.55	2.75	1.45	0.13	0.32	91.65	97.28	2.72	1.10
Eutheria		5.72e+06	11.96	49.78	38.26	32	5.80	6.01	1.96	0.15	0.33	90.17	96.76	3.24	1.18
Mammals		5.72e+06	8.30	48.98	42.72	34	7.28	7.48	2.42	0.15	0.30	90.86	97.27	2.73	0.91

Table 1.5: Summary statistics of sitewise estimates for all species groups with the conservative filter applied. Columns under the “ ω_{ML} Below / Above” heading measure the percentage of sites with ω_{ML} below or above the indicated value. Med.—median, Const.—constant, Syn.—synonymous, Nsyn.—non-synonymous, BL—branch length.

Name	Filter	Positively Selected Sites (%)								$P_{\chi^2_1} < 0.1$, %			$P_{\chi^2_1} < 0.05$, %		
		$P_{\chi^2_1} < 0.1$		$P_{\chi^2_1} < 0.05$		$P_{\chi^2_1} < 0.01$		FDR< 0.05		Neg.	Neut.	Pos.	Neg.	Neut.	Pos.
Primates	Conservative	45179	(0.73)	25710	(0.41)	7661	(0.12)	50	(0.001)	33.89	65.38	0.73	15.88	83.70	0.41
Atlantogenata		8143	(0.20)	3852	(0.09)	757	(0.02)	0	(0.000)	46.96	52.84	0.20	23.75	76.15	0.09
HMRD		6538	(0.13)	3040	(0.06)	534	(0.01)	0	(0.000)	63.74	36.13	0.13	37.42	62.52	0.06
Sparse Glires		7233	(0.14)	3316	(0.06)	644	(0.01)	0	(0.000)	70.34	29.52	0.14	49.07	50.87	0.06
HQ Mammals		29344	(0.46)	16374	(0.26)	4548	(0.07)	0	(0.000)	74.87	24.67	0.46	61.55	38.19	0.26
Glires		11155	(0.19)	5581	(0.10)	1221	(0.02)	0	(0.000)	78.93	20.88	0.19	67.92	31.98	0.10
Laurasiatheria		29058	(0.54)	17617	(0.33)	5944	(0.11)	41	(0.001)	78.31	21.15	0.54	68.74	30.93	0.33
Sparse Mammals		7953	(0.14)	3913	(0.07)	857	(0.02)	0	(0.000)	81.99	17.87	0.14	75.28	24.65	0.07
Eutheria		35270	(0.62)	24234	(0.42)	11006	(0.19)	999	(0.017)	89.00	10.38	0.62	86.54	13.04	0.42
Mammals		29075	(0.51)	19900	(0.35)	9025	(0.16)	781	(0.014)	90.61	8.88	0.51	88.54	11.11	0.35

Table 1.6: Proportions of sites subject to positive, purifying and neutral selection at various LRT_{SLR} thresholds. The Benjamini-Hochberg method [Benjamini & Hochberg, 1995] was used to identify the LRT_{SLR} threshold at which $FDR < 0.05$. For columns under the headings “ $P_{\chi_1^2} < 0.1$, %” and “ $P_{\chi_1^2} < 0.05$, %”, Pos. and Neg. are the percentage of sites with significant evidence for positive and negative selection, respectively, and Neut. is the percentage of “neutral” sites not showing significant evidence for non-neutral selection.

1.4.4 Modeling the global distribution of sitewise selective pressures

Species Set	Data Type	Log-normal		Gamma		Exponential		Beta		Weibull	
		$\bar{\omega}$	% > 1	$\bar{\omega}$	% > 1	$\bar{\omega}$	% > 1	$\bar{\omega}$	% > 1	$\bar{\omega}$	% > 1
Primates	ω_{ML}	0.11	1.53	0.25	7.31	0.25	1.82	0.25	0.00	0.14	2.96
Glires		0.15	2.07	0.16	3.35	0.16	0.16	0.20	0.00	0.12	2.56
Laurasiatheria		0.33	3.52	0.20	5.34	0.20	0.74	0.23	0.00	0.19	4.08
Atlantogenata		0.04	0.59	0.15	3.33	0.15	0.12	0.20	0.00	0.07	1.30
Eutheria		0.72	6.10	0.20	4.62	0.20	0.64	0.24	0.00	0.22	5.18
Mammalia		0.77	6.57	0.19	4.26	0.19	0.57	0.23	0.00	0.22	5.16
Sparse Glires		0.06	0.87	0.13	2.64	0.13	0.06	0.18	0.00	0.08	1.46
Sparse Mammalia		0.20	2.64	0.15	2.85	0.15	0.11	0.19	0.00	0.13	2.74
Primates	CI _{95%}	0.40	4.09	0.42	4.56	0.37	6.83	0.42	0.00	0.41	5.55
Glires		0.21	0.14	0.21	0.17	0.18	0.44	0.21	0.00	0.20	0.27
Laurasiatheria		0.22	0.95	0.23	0.45	0.22	1.05	0.23	0.00	0.23	0.64
Atlantogenata		0.30	0.58	0.32	0.55	0.26	2.14	0.32	0.00	0.30	1.26
Eutheria		0.19	2.28	0.18	0.79	0.18	0.42	0.18	0.00	0.18	1.32
Mammalia		0.18	2.35	0.18	0.74	0.17	0.31	0.17	0.00	0.17	1.27
Sparse Glires		0.23	0.14	0.24	0.24	0.20	0.67	0.25	0.00	0.23	0.43
Sparse Mammalia		0.16	0.10	0.17	0.09	0.15	0.13	0.17	0.00	0.16	0.11

Table 1.7: Mean ω and the percentage of sites with $\omega > 1$ based on maximum-likelihood fits of parametric distributions to sitewise estimates. For each species set and each one of five distribution types (log-normal, gamma, exponential, beta, and weibull) 100 replicate datasets of 1 million sites were sampled with replacement from the genome-wide dataset and the maximum likelihood distribution parameters were numerically optimized (see text for details). Columns show, for each distribution, the median value across 100 replicates of mean ω ($\bar{\omega}$) and the probability mass with $\omega > 1$, expressed as a percentage (% > 1). The top eight rows show the results based on fitting parameters to sitewise ω_{ML} estimates, and the bottom eight rows show the results based on fitting parameters to sitewise CI_{95%} estimates. Note the greater consistency of $\bar{\omega}$ and % > 1 across distribution types for the CI_{95%}-based fits.

We used the `fitdistr` function of the MASS package for R to fit five distributions (gamma, lognormal, beta, Weibull, and exponential) to the vertebrate dN/dS values and subsequently calculated Akaike's Information Criterion (AIC) for each fit. For all optimizations, a constant value of 0.001 was added to sites where $dN/dS = 0$ in order to satisfy the optimizers requirement that the probability functions have a defined value for all input data. Similarly, sites with $dN/dS \leq 1$ were excluded from the analysis for the beta optimization. All distributions were also separately fit to the subset of sites with $dN/dS \leq 1$; the AIC values from these optimizations were used to compare the fit of the beta distribution to the others.

The `fitdistr` produced the following optimized parameters for each function: gamma (shape=0.271, rate=1.203), lognormal (meanlog=-4.079, sdlog=2.863), beta (shape1=0.257, shape2=1.431), Weibull (shape=0.3882, scale=0.07151) exponential (rate=4.441). The beta distribution yielded the lowest AIC when compared to the fit of other distributions to the subset of sites where $dN/dS \leq 1$ (-2.33e7 versus the next best equivalent AIC of -2.11e7 for the lognormal). Of the distributions which were fit to the whole dataset, the lognormal distribution yielded the lowest AIC (-2.11e7), followed by gamma (-2.03e7) and exponential (-6.45e6).

1.4.5 Simulations to evaluate the power to detect positive selection and estimate selective pressures

1.4.6 Evaluation of the effect of GC content, recombination rate, and codon usage on sitewise dN/dS estimates and the detection of positive selection

Species Set	Distribution	AIC	<i>d</i> AIC	Parameter A	Parameter B
Primates	Beta	161168.45	0.00	1.78	2.50
	Lognormal	217743.70	56575.25	-1.14	0.65
	Gamma	231082.15	13338.45	2.12	5.06
	Weibull	242149.95	11067.80	1.34	0.45
	Exponential	261904.40	19754.45	2.68	
Glires	Lognormal	312788.30	0.00	-1.76	0.59
	Beta	332776.25	19987.95	1.57	5.75
	Gamma	341872.95	9096.70	1.70	8.02
	Weibull	364256.80	22383.85	1.15	0.21
	Exponential	385083.15	20826.35	5.42	
Laurasiatheria	Lognormal	514030.30	0.00	-1.80	0.77
	Beta	528667.45	14637.15	1.25	4.27
	Gamma	558537.00	29869.55	1.49	6.52
	Weibull	570535.20	11998.20	1.12	0.23
	Exponential	575734.00	5198.80	4.56	
Atlantogenata	Beta	109348.25	0.00	2.37	4.93
	Lognormal	119888.05	10539.80	-1.34	0.53
	Gamma	126416.00	6527.95	2.75	8.72
	Weibull	143678.60	17262.60	1.33	0.33
	Exponential	175474.60	31796.00	3.84	
Eutheria	Lognormal	1180885.50	0.00	-2.40	1.20
	Weibull	1270446.50	89561.00	0.80	0.16
	Gamma	1295309.50	24863.00	0.80	4.35
	Beta	1307444.50	12135.00	0.69	3.16
	Exponential	1308964.50	1520.00	5.46	
Mammalia	Lognormal	1310778.00	0.00	-2.51	1.26
	Weibull	1403090.50	92312.50	0.78	0.15
	Gamma	1433878.50	30788.00	0.75	4.30
	Beta	1456833.00	22954.50	0.65	3.11
	Exponential	1459667.50	2834.50	5.77	
Sparse Glires	Beta	161165.45	0.00	2.04	6.12
	Lognormal	161264.00	98.55	-1.60	0.53
	Gamma	176568.30	15304.30	1.99	8.23
	Weibull	198910.90	22342.60	1.20	0.24
	Exponential	225609.40	26698.50	5.00	
Sparse Mammalia	Lognormal	403243.50	0.00	-2.09	0.68
	Gamma	447431.20	44187.70	1.31	7.74
	Beta	450936.70	3505.50	1.18	5.70
	Weibull	462813.80	11877.10	1.06	0.16
	Exponential	471324.15	8510.35	6.67	

Table 1.8: AIC values and parameters for maximum-likelihood fits of parametric distributions to sitewise $CI_{95\%}$ estimates. Distributions were fit to 100 replicate datasets for each species set as in Table 1.7. For each species set and distribution type, the median Akaike information criterion (AIC) and parameter estimates are shown. Distributions are sorted according to their median AIC value (where a lower AIC corresponds to a better fit to the data), and the difference in AIC to the next-best fitting distribution is displayed (*d*AIC). The lognormal and beta distributions are ranked first or second in the mammalian superorder subgroups, while lognormal, weibull and gamma distributions fit the Eutheria and Mammalia datasets best. The named parameters corresponding to parameters A and B for each distribution are as follows: lognormal (A=meanlog, B=sdlog), weibull (A=shape, B=scale), gamma (A=shape, B=rate [where rate=1/scale]), beta (A=shape1 [α], B=shape2 [β]), exponential (A=rate [λ]).

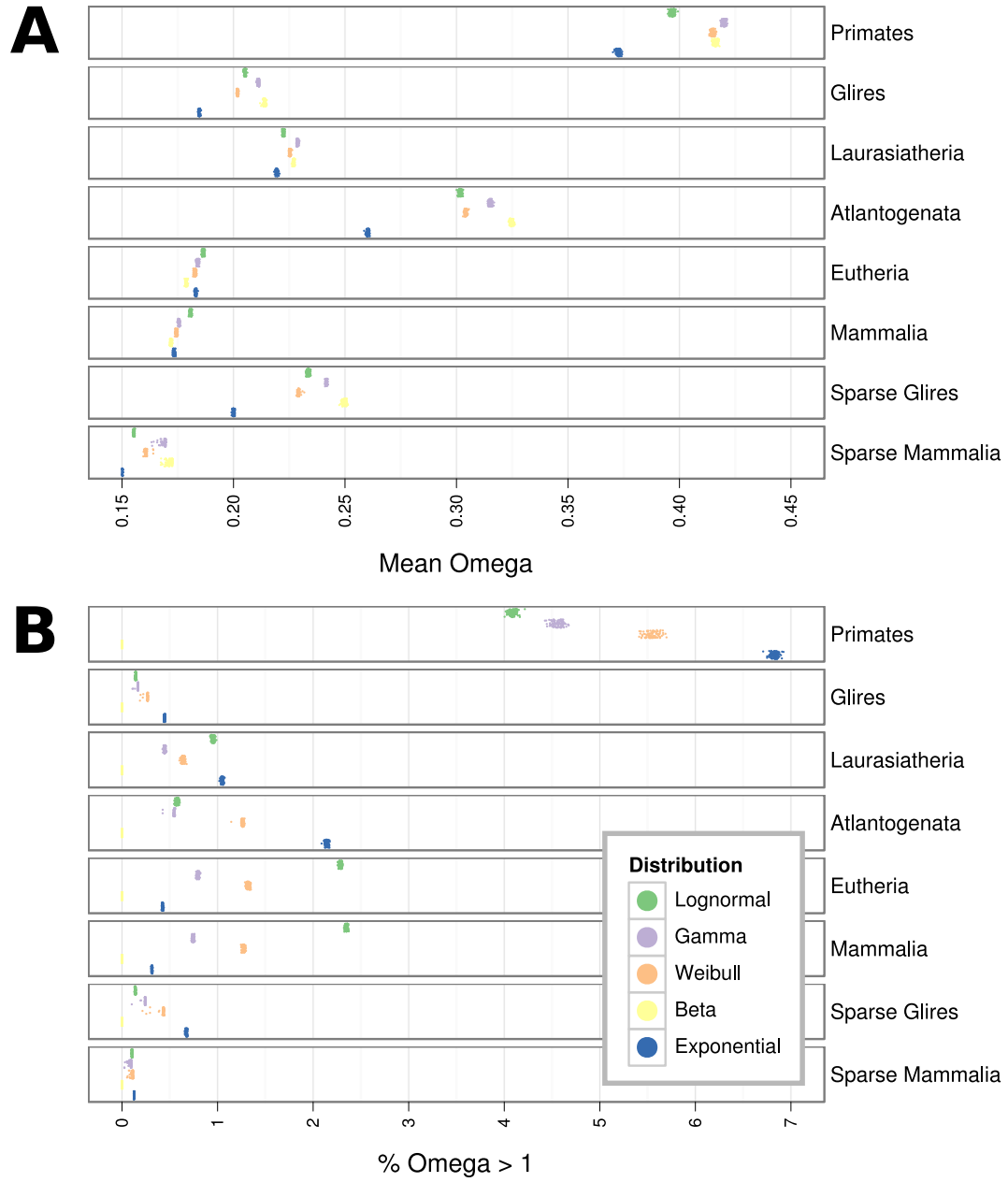


Figure 1.9: The mean value (A, Mean Omega) and the percentage of probability density with $\omega > 1$ (B, Omega > 1) from maximum likelihood fits of parametric distributions to sitewise $CI_{95\%}$ estimates. Each point represents the maximum likelihood fit of one distribution to 1 million points sampled from the genome-wide dataset with replacement; 100 such fits were generated for each distribution and species set. Note that the beta distribution is only defined on the interval (0,1), so the percentage of sites with $\omega > 1$ was always zero.

Variable	Species Group	Quantile	Sites	Med. BL	NSC _{10%}	ω_{ML} < 0.5	PSC _{10%}	ω_{ML} > 1.5	Recomb., cM		GC	Substitutions %				
									Male	Female		Total	CpG	W-S	S-W	Nsyn
gc	Mammalia	(0,0.05]	315984	6.176	88.131	89.000	0.715	1.343	0.645	1.242	0.336	0.387	0.010	0.198	0.180	0.347
		(0.05,0.275]	1408253	6.583	86.932	87.675	0.823	1.508	0.762	1.477	0.371	0.415	0.013	0.206	0.197	0.360
		(0.275,0.5]	1389575	7.127	86.139	86.870	0.873	1.628	0.898	1.709	0.413	0.450	0.019	0.206	0.224	0.355
		(0.5,0.725]	1379927	7.530	87.514	88.229	0.747	1.466	1.012	1.815	0.469	0.463	0.029	0.181	0.253	0.340
		(0.725,0.95]	1397262	7.599	89.893	90.715	0.489	1.077	1.144	1.822	0.543	0.431	0.037	0.137	0.257	0.320
		(0.95,1]	312449	8.205	91.843	92.698	0.253	0.699	1.720	1.223	0.622	0.430	0.043	0.126	0.260	0.312
decodeM	Mammalia	(0.05,0.275]	1701616	6.923	86.696	87.790	0.800	1.578	0.076	1.143	0.450	0.424	0.023	0.170	0.231	0.351
		(0.275,0.5]	1397371	7.061	87.674	88.451	0.743	1.405	0.448	1.467	0.441	0.425	0.022	0.178	0.225	0.344
		(0.5,0.725]	1393633	7.038	88.395	89.098	0.672	1.300	0.866	1.767	0.441	0.425	0.023	0.180	0.221	0.334
		(0.725,0.95]	1372925	7.667	88.553	89.025	0.643	1.265	1.874	2.271	0.462	0.462	0.028	0.193	0.242	0.337
		(0.95,1]	304151	8.359	89.671	90.113	0.505	1.049	4.886	2.130	0.512	0.495	0.036	0.194	0.265	0.342
decodeF	Mammalia	(0,0.05]	304114	7.693	88.210	88.987	0.515	1.152	0.853	0.001	0.500	0.463	0.032	0.174	0.257	0.350
		(0.05,0.275]	1394890	6.946	87.068	88.057	0.762	1.495	0.799	0.466	0.444	0.428	0.023	0.175	0.230	0.349
		(0.275,0.5]	1393061	6.965	87.831	88.632	0.742	1.409	0.742	1.116	0.435	0.424	0.022	0.181	0.221	0.339
		(0.5,0.725]	1386168	7.306	87.545	88.278	0.771	1.472	0.893	1.833	0.456	0.443	0.025	0.182	0.236	0.347
		(0.725,0.95]	1382191	7.397	88.800	89.395	0.611	1.210	1.324	2.892	0.459	0.442	0.026	0.184	0.231	0.330
		(0.95,1]	309272	7.619	88.451	88.896	0.671	1.302	1.764	4.780	0.465	0.455	0.028	0.189	0.239	0.343

Table 1.9

Variable	Species Group	Quantile	Sites Sites	Med. BL	$P_{\chi^2_1} < 0.1$ Neg.	$\omega_{ML} < 0.5$	$P_{\chi^2_1} < 0.1$ Pos.	$\omega_{ML} > 1.5$	Recombination		GC	WS	CpG	Nonsyn.	Syn.	
gc	Primates	(0,0.05]	292632	0.656	25.449	86.235	0.849	5.405	0.645	1.234	0.336	0.420	0.010	0.216	0.194	0.357
		(0.05,0.275]	1305896	0.688	24.330	85.190	0.923	5.824	0.771	1.488	0.372	0.439	0.013	0.217	0.208	0.366
		(0.275,0.5]	1289390	0.740	26.741	84.804	0.984	5.994	0.912	1.728	0.414	0.469	0.020	0.215	0.234	0.358
		(0.5,0.725]	1283434	0.797	34.863	85.763	0.882	5.444	1.033	1.815	0.470	0.483	0.030	0.189	0.264	0.342
		(0.725,0.95]	1296483	0.823	43.732	88.127	0.655	4.398	1.156	1.825	0.544	0.453	0.038	0.145	0.270	0.323
		(0.95,1]	288995	0.937	54.446	89.725	0.452	3.418	1.738	1.203	0.622	0.452	0.045	0.134	0.273	0.313
decodeM	Primates	(0.05,0.275]	1575779	0.731	29.090	85.704	0.923	5.801	0.077	1.146	0.450	0.446	0.024	0.179	0.243	0.356
		(0.275,0.5]	1299507	0.740	30.437	86.009	0.859	5.480	0.452	1.481	0.442	0.449	0.023	0.188	0.237	0.350
		(0.5,0.725]	1289984	0.737	32.063	86.581	0.810	5.155	0.876	1.769	0.441	0.447	0.024	0.191	0.232	0.338
		(0.725,0.95]	1278924	0.823	38.578	86.317	0.796	4.948	1.900	2.276	0.464	0.482	0.029	0.201	0.252	0.339
		(0.95,1]	282104	0.981	48.091	87.212	0.629	4.176	4.951	2.133	0.512	0.512	0.037	0.200	0.275	0.342
decodeF	Primates	(0,0.05]	282128	0.859	40.030	86.187	0.719	4.931	0.872	0.001	0.500	0.484	0.033	0.183	0.268	0.354
		(0.05,0.275]	1294422	0.746	29.687	85.912	0.880	5.630	0.818	0.466	0.446	0.450	0.024	0.184	0.243	0.353
		(0.275,0.5]	1293324	0.730	30.631	86.244	0.849	5.386	0.772	1.123	0.436	0.447	0.023	0.191	0.233	0.345
		(0.5,0.725]	1284474	0.774	33.634	85.823	0.895	5.438	0.886	1.840	0.456	0.464	0.026	0.191	0.247	0.351
		(0.725,0.95]	1285566	0.789	36.130	86.716	0.769	4.957	1.337	2.903	0.460	0.462	0.027	0.193	0.242	0.334
		(0.95,1]	286384	0.800	37.262	86.325	0.802	4.950	1.769	4.799	0.463	0.475	0.029	0.198	0.247	0.346

Table 1.10

Multiple lines of evidence have lent support to the hypothesis that GC-biased gene conversion (BGC) has been a major force in the evolution of mammalian genomes [Galtier et al 2001 PMID:11693127, Galtier 2003 PMID:XYZ, Dreszer et al 2007 PMID:17785536]. Both empirical and theoretical results have shown that BGC can significantly affect patterns of observed substitutions in both selectively neutral and functionally constrained sites [Galtier et al 2009 PMID:19027980, Berglund et al 2009 PMID:19175294]. Recently, Ratnakumar et al. [2010, PMID:20643747] re-analyzed the dataset of positively-selected genes from Kosiol et al. [2008, PMID:18670650] for signatures of BGC and found that up to 20% of cases of identified elevated dN/dS ratios could be due to BGC rather than adaptive evolution. However, the strongest signals of BGC were found only in genes showing signals of positive selection along short branches in the phylogenetic tree using so-called branch-site models of evolution; when the authors looked for similar BGC signatures in genes with evidence for positive selection at specific sites throughout the mammalian tree (e.g., genes with significant LRTs for PAMLs sites model) they found no evidence for a strong BGC influence [Ratnakumar et al. 2010 PMID:20643747].

The above evidence suggests that although BGC has the potential to produce misleading signals of branch-specific positive selection near recombination hotspots, the positively-selected sites we detected should not be strongly influenced by the non-adaptive effects of BGC since the dN/dS level detected by SLR is estimated from across the entire input phylogeny [Massingham 2005 PMID:15654091]. This is consistent with the observation that recombination hotspots (where most recombination in humans and other mammals occurs [Myers et al. 2005 PMID:16224025]) tend not to be maintained over long evolutionary periods, although larger-scale recombination rates are likely more conserved [Winckler et al 2005 PMID:15705809]. Still, due to the potential confounding implications of BGC on the interpretation of signals of positive selection, we found it worthwhile to empirically test for any BGC effect on our data.

The BGC model predicts a recombination-associated drive towards the fixation of GC alleles at heterozygous sites, resulting in an expected correlation between AT to GC (or weak-to-strong, W-S) mutational bias and recombination rate [Galtier and Duret 2007, PMID:17418442]. This bias can lead to elevated dN/dS estimates in coding regions, particularly in GC-rich regions where W-S mutations are more likely to result in nonsynonymous changes [Berglund et al 2009]. Ratnakumar and colleagues identified three ways of distinguishing potential BGC effects from true signals of positive selection in protein-coding regions: (a) positive selection is not expected on its own to result in a strong W-S bias, (b)

a BGC-associated W-S biased mutation pattern should extend to noncoding sites flanking the affected coding region, and (c) BGC is associated with recombination hotspots and regions of high recombination rates (and most strongly with male-specific rates) while there is no empirical evidence linking positive selection with higher recombination rates in mammals, although natural selection should theoretically be more efficient in regions of high recombination [Ratnakumar et al. 2010, PMID:20643747]. We could not use (a) or (b) to detect possible BGC influence since we did not calculate inferred ancestral mutations for either the coding or flanking noncoding regions of the mammalian gene families studied here. Instead, we turned to point (c) and tested for a correlation between signals of positive selection and an increase in recombination rates, especially the male-specific rate and in regions of high GC content. The predictions of the BGC hypothesis suggest that if our sitewise data do contain a strong BGC influence, then the positively-selected sites we detected would be expected to be associated with regions of high male-specific recombination.

We combined the sitewise codon data with male, female, and sex-averaged recombination rates derived from the deCODE map (using rates averaged over genomic bins of 1Mb downloaded from the UCSC human genome browser hg19 release) and human GC content calculated in 10-kb windows and analyzed sites within various quantiles of GC content, mean recombination rate, and sitewise statistics. Supplementary Table S17.13 contains summaries for each subset. The LRT statistic section shows that sites with higher LRT statistics (which corresponds to weaker purifying selection when the value is below zero and stronger positive selection when the value is above zero) show decreasing recombination rates; this trend holds true even for the highest quantile (mean signed_lrt between 3.648 and 108.850), which is composed entirely of sites with evidence for positive selection. In other words, the bulk of positively-selected sites are in regions of lower than average male recombination rates – exactly opposite what would be expected in the face of strong BGC effects. The Male Recombination quantiles show a similar trend, with the mean dN/dS, mean signed LRT and the proportion of sites identified as positively-selected (pos_f) all consistently decreasing as the recombination rate increases. The GC content quantiles showed a slightly different pattern. Although the mean LRT decreased and male recombination increased monotonically with increasing GC content, the mean dN/dS and fraction of positive sites started low, increased to a maximum in the middle range of GC content, and decreased again in regions of high GC content. Thus, although the GC content quantiles were similar to the male recombination quantiles in their higher range (with similar

mean dN/dS, mean LRT, and pos.f values), they differed slightly in their lower range (with lower dN/dS and pos.f for low GC quantiles). Although the exact reason for such a pattern is unclear, it is consistent with the existence of altered or constrained selective or mutational dynamics at the extreme ends of the genomic distribution of GC content. As GC content has been shown to correlate with myriad structural and evolutionary features of mammalian genomes [Xia et al. 2009 PMID:19521505], the existence of other (possibly unrelated) confounding influences such as CpG mutability or isochore structure is likely.

Theoretical and empirical evidence pointed towards an increased sensitivity of dN/dS estimates to BGC influence in regions of high GC content, so we separated out the top 10% of sites by GC content and analyzed them according to quantiles of male recombination rate (Supplementary Table S17.13, High GC, Male Recombination). The middle four recombination quantiles showed a similar pattern to that observed for all GC contents, with mean LRT decreasing with increased male recombination and mean dN/dS and pos.f decreasing or hovering around values slightly lower than those observed across all GC contents (e.g., mean dN/dS in the 1-25% bin is 0.207 for the top 10% GC sites, but 0.249 for the same recombination bin across all sites). The highest recombination bin of the top 10% GC sites showed a strikingly different pattern, however, with mean dN/dS=0.348, mean LRT=-11.262, and pos.f=0.0338. These values suggest a strong shift towards higher dN/dS values and more positively-selected sites. This jump in values in the highest recombination bin is not seen in the highest male recombination bin across all GC contents (mean dN/dS=0.207, mean LRT=-16.616, pos.f=0.00932) or for the highest female recombination bin for the top 10% of GC sites (mean dN/dS=0.164, mean LRT=-18.475, pos.f=0.00449). Although the small number of sites in the bin of interest compared to other bins suggests possible stochastic artifacts, the shift is dramatic, directly opposite to the trends observed for the female recombination rates and for male recombination rates in regions of lower GC content, and is in agreement with the BGC prediction of elevated dN/dS estimates in regions of high GC content and male-specific recombination rates. This evidence raises the interesting possibility that BGC may have a detectable, if rather minor, impact on sitewise dN/dS estimates across the mammalian phylogeny. It is highly unlikely, however, that any such effect – which in our analysis was only detectable in 0.05% of sites with the most extreme GC content and recombination rates – has contaminated our codon-specific estimates with more than a negligible amount of noise resulting from the neutral but biased process of BGC.

1.5 Conclusions

[To cite: ? — Showed, through constraint analysis of various sequence types, that there is higher selective constraint in 4-fold sites in priamtes compared to murids. Quote: “It is well established that in several organisms, mutations at 4-fold sites are selected against (Chamary et al. 2006; Rocha 2006; Drummond and Wilke 2008) and as a consequence the dN/ds ratio, which has been frequently used to detect the strength and direction of selection (e.g., Dorus et al. 2004; Wang et al. 2006), may be underestimated. Our result of higher 4-fold constraint in hominids suggests that this bias more strongly affects hominid estimates and it may well exceed 20%.”]

[To cite: ?? — The Keightley et al. 2011 paper (ABC to estimate mutation rate parameters) cited Ohta 1993, 1995 and Eory et al. 2010 for the effective population size and efficacy of selection in primates vs. murids]

[To cite: ? — Wolf et al. GBE 2009, used pairwise dN dS counts to try to show that trends in dN/dS ratios are a result of branch length, at least when calculated in a pairwise fashion. Slightly unconvincing stuff... could be cited as somehow relating to the discussion regarding eff. pop. size, branch length, and selection]

[To cite: ? — Berglund et al. 2009 looked at hotspots of biased substitutions in humans. Showed that exons with accelerated rates in humans have a tendency towards clusters of AT-to-GC (weak-to-strong) substitutions. Did some simulations showing that this effect is strongest in GC-poor regions, though the impact on overall dN/dS is probably minimal (e.g., genes with overall high dN/dS didn’t show BGC, only the most accelerated exons did) and the effect on dN/dS is highest in high-GC regions. The most-accelerated exons tend to reside in high-male (but not female) recombination, and j50kb from hotspots. Upshot: these biased clusters seem to show up in isolated regions (exons), rather than spread throughout entire genes. Probably not a huge impact on overall apparent constraint.]

[To cite: ? — Duret and Arndt 2008 use nonreversible nucleotide models to estimate NEUTRAL rates correlated with recombination, GC, and GC*. Lots of stuff here, but the important bits: overall mutation rate increases with increasing GC content (due to overall higher rates of S-W substitution); recombination should have a strong impact on W-S substitution, but weak impact on S-W substitutions; CpG deamination varies by factor of two, very low in GC-poor regions and very high in GC-rich ones.]

[To cite: ? — Galtier et al. TRIG 2009 is similar to Berglund et al. in many ways – find accelerated exons in a primate branch, and identify significantly higher male recombination rates there. The number of accelerated exons is small – 100 in each of four branches – and

not all of these accelerated exons showed strongly elevated dN/dS ratios. Only 19 exons at the 1% level. However, they do some nice modeling (mostly in the supp. material) which shows that the effect of BCG on dN/dS ratio at different GC contents – it has more effect in GC-rich genes.]

[To cite: ? — Capra and Pollard quantified BDS (biased divergent substitutions) across metazoans, additionally using recombination rate data. Dog has the strongest, mouse has the weakest BDS scores. (This could be due to lower rec. rate in mouse, e.g. Coop and Przeworski 2006)]

[To cite: ? — Nordborg et al. 1996 (Genet. Res.) modeled the effect of background selection on variation in neutral linked loci. They showed that weakly selected mutations, rather than strongly selected ones, are more likely to produce regional patterning of variation in response to local recombination rate. Should have a large effect in *Drosophila* but small effect in mammals, though in mammals “local reductions in regions of reduced recombination might be detectable.”]

[To cite: ? — Chun and Fay 2011 (PLoS Gen) looked at neutral and deleterious SNP density according to local recombination rate, showing that in ‘hitchhiking’ regions there are fewer neutral, but as many deleterious, polymorphisms. That stuff is boring, but they also show that the deleterious SNP density stays constant throughout the range of recombination rates, while the neutral and synonymous SNP density decreases. Thus, slightly deleterious mutations are less effectively purged in regions of low recombination.]

[To cite: ? — Bullaughey et al. (2008, Gen. Res.) looked at gene-wide dN/dS ratios in primates and recombination rates. They found no significant correlation between broad- or fine-scale recomb. rates and rates of protein evolution, **once GC content is taken into account**.]

[To cite: ? — Spencer et al. (2006 PLoS Gen) Quote: “In short, while there is a strong relationship between recombination and GC content, most of the relationship is explained by scales broader than recombination hotspots (16 to 256 kb; unpublished data) and may well result from interactions of both factors with additional processes such as chromatin organisation or replication timing. Similar arguments apply to the question of whether a GC bias in recombination-associated mutation can explain the relationship between GC content and recombination.”]

[...]

Bibliography

- ANISIMOVA, M., BIELAWSKI, J. & YANG, Z. (2002). Accuracy and power of bayes prediction of amino acid sites under positive selection. *Mol Biol Evol*, **19**, 950–8. [5](#)
- ANISIMOVA, M., NIELSEN, R. & YANG, Z. (2003). Effect of recombination on the accuracy of the likelihood method for detecting positive selection at amino acid sites. *Genetics*, **164**, 1229–36. [5](#)
- AVEROF, M., ROKAS, A., WOLFE, K. & SHARP, P. (2000). Evidence for a high frequency of simultaneous double-nucleotide substitutions. *Science*, **287**, 1283–6. [28](#)
- BAKEWELL, M., SHI, P. & ZHANG, J. (2007). More genes underwent positive selection in chimpanzee evolution than in human evolution. *Proc Natl Acad Sci U S A*, **104**, 7489–94. [9](#)
- BAZYKIN, G., KONDRASHOV, F., OGURTSOV, A., SUNYAEV, S. & KONDRASHOV, A. (2004). Positive selection at sites of multiple amino acid replacements since rat-mouse divergence. *Nature*, **429**, 558–62. [19](#)
- BEISSWANGER, S. & STEPHAN, W. (2008). Evidence that strong positive selection drives neofunctionalization in the tandemly duplicated polyhomeotic genes in drosophila. *Proc Natl Acad Sci U S A*, **105**, 5447–52. [9](#)
- BENJAMINI, Y. & HOCHBERG, Y. (1995). Controlling the false discovery rate: a practical and powerful approach to multiple testing. *Journal of the Royal Statistical Society. Series B (Methodological)*, **57**, 289–300. [33](#), [37](#), [40](#)
- CALLAHAN, B., NEHER, R., BACHTROG, D., ANDOLFATTO, P. & SHRAIMAN, B. (2011). Correlated evolution of nearby residues in drosophilid proteins. *PLoS Genet*, **7**, e1001315. [19](#)

BIBLIOGRAPHY

- CASOLA, C. & HAHN, M. (2009). Gene conversion among paralogs results in moderate false detection of positive selection using likelihood methods. *J Mol Evol*, **68**, 679–87. [9](#)
- CHURAKOV, G., KRIEGS, J., BAERTSCH, R., ZEMANN, A., BROSIUS, J. & SCHMITZ, J. (2009). Mosaic retroposon insertion patterns in placental mammals. *Genome Res*, **19**, 868–75. [23](#)
- CLARK, A., GLANOWSKI, S., NIELSEN, R., THOMAS, P., KEJARIWAL, A., TODD, M., TANENBAUM, D., CIVELLO, D., LU, F., MURPHY, B., FERRIERA, S., WANG, G., ZHENG, X., WHITE, T., SNINSKY, J., ADAMS, M. & CARGILL, M. (2003). Inferring nonneutral evolution from human-chimp-mouse orthologous gene trios. *Science*, **302**, 1960–3. [13](#)
- COCK, P., FIELDS, C., GOTO, N., HEUER, M. & RICE, P. (2010). The sanger FASTQ file format for sequences with quality scores, and the Solexa/Illumina FASTQ variants. *Nucleic Acids Res*, **38**, 1767–71. [10](#)
- TOCITE** (2011). Citation will be inserted at a later point in time. [3](#), [12](#), [13](#)
- ENCODE PROJECT CONSORTIUM (2007). Identification and analysis of functional elements in 1% of the human genome by the ENCODE pilot project. *Nature*, **447**, 799–816. [4](#), [11](#)
- FINN, R., MISTRY, J., TATE, J., COGGILL, P., HEGER, A., POLLINGTON, J., GAVIN, O., GUNASEKARAN, P., CERIC, G., FORSLUND, K., HOLM, L., SONNHAMMER, E., EDDY, S. & BATEMAN, A. (2010). The pfam protein families database. *Nucleic Acids Res*, **38**, D211–22. [31](#)
- FLETCHER, W. & YANG, Z. (2010). The effect of insertions, deletions, and alignment errors on the branch-site test of positive selection. *Mol Biol Evol*, **27**, 2257–67. [9](#)
- GREEN, P. (2007). 2x genomes—does depth matter? *Genome Res*, **17**, 1547–9. [5](#)
- HAN, M., DEMUTH, J., MCGRATH, C., CASOLA, C. & HAHN, M. (2009). Adaptive evolution of young gene duplicates in mammals. *Genome Res*, **19**, 859–67. [14](#)
- HUBBARD, T., AKEN, B., BEAL, K., BALLESTER, B., CACCAMO, M., CHEN, Y., CLARKE, L., COATES, G., CUNNINGHAM, F., CUTTS, T., DOWN, T., DYER, S., FITZGERALD, S., FERNANDEZ-BANET, J., GRAF, S., HAIDER, S., HAMMOND, M.,

BIBLIOGRAPHY

- HERRERO, J., HOLLAND, R., HOWE, K., HOWE, K., JOHNSON, N., KAHARI, A., KEEFE, D., KOKOCINSKI, F., KULESHA, E., LAWSON, D., LONGDEN, I., MELSOPP, C., MEGY, K., MEIDL, P., OUVERDIN, B., PARKER, A., PRILIC, A., RICE, S., RIOS, D., SCHUSTER, M., SEALY, I., SEVERIN, J., SLATER, G., SMEDLEY, D., SPUDICH, G., TREVANION, S., VILELLA, A., VOGEL, J., WHITE, S., WOOD, M., COX, T., CURWEN, V., DURBIN, R., FERNANDEZ-SUAREZ, X., FLICEK, P., KASPRZYK, A., PROCTOR, G., SEARLE, S., SMITH, J., URETA-VIDAL, A. & BIRNEY, E. (2007). Ensembl 2007. *Nucleic Acids Res*, **35**, D610–7. [10](#)
- HUBISZ, M., LIN, M., KELLIS, M. & SIEPEL, A. (2011). Error and error mitigation in low-coverage genome assemblies. *PLoS One*, **6**, e17034. [10](#), [11](#)
- JAFFE, D., BUTLER, J., GNERRE, S., MAUCELI, E., LINDBLAD-TOH, K., MESIROV, J., ZODY, M. & LANDER, E. (2003). Whole-genome sequence assembly for mammalian genomes: Arachne 2. *Genome Res*, **13**, 91–6. [6](#), [10](#)
- KIRCHER, M., STENZEL, U. & KELSO, J. (2009). Improved base calling for the illumina genome analyzer using machine learning strategies. *Genome Biol*, **10**, R83. [6](#)
- KOSIOL, C., HOLMES, I. & GOLDMAN, N. (2007). An empirical codon model for protein sequence evolution. *Mol Biol Evol*, **24**, 1464–79. [28](#)
- KOSIOL, C., VINAR, T., DA FONSECA, R., HUBISZ, M., BUSTAMANTE, C., NIELSEN, R. & SIEPEL, A. (2008). Patterns of positive selection in six mammalian genomes. *PLoS Genet*, **4**, e1000144. [13](#)
- LINDBLAD-TOH, K., WADE, C.M., MIKKELSEN, T.S., KARLSSON, E.K., JAFFE, D.B., KAMAL, M., CLAMP, M., CHANG, J.L., KULBOKAS, E.J., ZODY, M.C., MAUCELI, E., XIE, X., BREEN, M., WAYNE, R.K., OSTRANDER, E.A., PONTING, C.P., GALIBERT, F., SMITH, D.R., DEJONG, P.J., KIRKNESS, E., ALVAREZ, P., BIAGI, T., BROCKMAN, W., BUTLER, J., CHIN, C.W., COOK, A., CUFF, J., DALY, M.J., DECAPRIO, D., GNERRE, S., GRABHERR, M., KELLIS, M., KLEBER, M., BARDELEBEN, C., GOODSTADT, L., HEGER, A., HITTE, C., KIM, L., KOEPFLI, K.P., PARKER, H.G., POLLINGER, J.P., SEARLE, S.M.J., SUTTER, N.B., THOMAS, R., WEBBER, C., BALDWIN, J., BROAD SEQUENCING PLATFORM MEMBERS & LANDER, E.S. (2005). Genome sequence, comparative analysis and haplotype structure of the domestic dog. *Nature*, **438**, 803–819. [3](#)

BIBLIOGRAPHY

- LINDBLAD-TOH, K., GARBER, M., ZUK, O. & ,ET AL. (64 CO-AUTHORS) (2011). A high-resolution map of evolutionary constraint in the human genome based on 29 eutherian mammals (in press). *Nature*, **0**, 0. [4](#)
- LYNCH, M. & CONERY, J. (2000). The evolutionary fate and consequences of duplicate genes. *Science*, **290**, 1151–5. [12](#)
- MALLICK, S., GNERRE, S., MULLER, P. & REICH, D. (2009). The difficulty of avoiding false positives in genome scans for natural selection. *Genome Res*, **19**, 922–33. [9](#), [27](#)
- MARGULIES, E., VINSON, J., NISC COMPARATIVE SEQUENCING PROGRAM, MILLER, W., JAFFE, D., LINDBLAD-TOH, K., CHANG, J., GREEN, E., LANDER, E., MULLIKIN, J. & CLAMP, M. (2005). An initial strategy for the systematic identification of functional elements in the human genome by low-redundancy comparative sequencing. *Proc Natl Acad Sci U S A*, **102**, 4795–800. [3](#)
- MARGULIES, E., COOPER, G., ASIMENOS, G., THOMAS, D., DEWEY, C., SIEPEL, A., BIRNEY, E., KEEFE, D., SCHWARTZ, A., HOU, M., TAYLOR, J., NIKOLAEV, S., MONTOYA-BURGOS, J., LÖYTYNOJA, A., WHELAN, S., PARDI, F., MASSINGHAM, T., BROWN, J., BICKEL, P., HOLMES, I., MULLIKIN, J., URETA-VIDAL, A., PATEN, B., STONE, E., ROSENBLOOM, K., KENT, W., BOUFFARD, G., GUAN, X., HANSEN, N., IDOL, J., MADURO, V., MASKERI, B., MCDOWELL, J., PARK, M., THOMAS, P., YOUNG, A., BLAKESLEY, R., MUZNY, D., SODERGREN, E., WHEELER, D., WORLEY, K., JIANG, H., WEINSTOCK, G., GIBBS, R., GRAVES, T., FULTON, R., MARDIS, E., WILSON, R., CLAMP, M., CUFF, J., GNERRE, S., JAFFE, D., CHANG, J., LINDBLAD-TOH, K., LANDER, E., HINRICHS, A., TRUMBOWER, H., CLAWSON, H., ZWEIG, A., KUHN, R., BARBER, G., HARTE, R., KAROLCHIK, D., FIELD, M., MOORE, R., MATTHEWSON, C., SCHEIN, J., MARRA, M., ANTONARAKIS, S., BATZOGLOU, S., GOLDMAN, N., HARDISON, R., HAUSSLER, D., MILLER, W., PACTER, L., GREEN, E. & SIDOW, A. (2007). Analyses of deep mammalian sequence alignments and constraint predictions for 1% of the human genome. *Genome Res*, **17**, 760–74. [3](#), [4](#)
- MARKOVA-RAINA, P. & PETROV, D. (2011). High sensitivity to aligner and high rate of false positives in the estimates of positive selection in the 12 drosophila genomes. *Genome Research*, **21**, 863–874. [27](#)
- MASSINGHAM, T. & GOLDMAN, N. (2005). Detecting amino acid sites under positive selection and purifying selection. *Genetics*, **169**, 1753–62. [4](#), [5](#), [28](#), [30](#), [36](#)

BIBLIOGRAPHY

- MOUSE GENOME SEQUENCING CONSORTIUM & MOUSE GENOME ANALYSIS GROUP (2002). Initial sequencing and comparative analysis of the mouse genome. *Nature*, **420**, 520–62. [3](#)
- MURPHY, W., PRINGLE, T., CRIDER, T., SPRINGER, M. & MILLER, W. (2007). Using genomic data to unravel the root of the placental mammal phylogeny. *Genome Res*, **17**, 413–21. [23](#)
- NIELSEN, R., BUSTAMANTE, C., CLARK, A., GLANOWSKI, S., SACKTON, T., HUBISZ, M., FLEDEL-ALON, A., TANENBAUM, D., CIVELLO, D., WHITE, T., J SNINSKY, J., ADAMS, M. & CARGILL, M. (2005). A scan for positively selected genes in the genomes of humans and chimpanzees. *PLoS Biol*, **3**, e170. [13](#)
- NIKOLAEV, S., MONTROYA-BURGOS, J., POPADIN, K., PARAND, L., MARGULIES, E., NATIONAL INSTITUTES OF HEALTH INTRAMURAL SEQUENCING CENTER COMPARATIVE SEQUENCING PROGRAM & ANTONARAKIS, S. (2007). Life-history traits drive the evolutionary rates of mammalian coding and noncoding genomic elements. *Proc Natl Acad Sci U S A*, **104**, 20443–8. [24](#)
- RAT GENOME SEQUENCING PROJECT CONSORTIUM (2004). Genome sequence of the brown norway rat yields insights into mammalian evolution. *Nature*, **428**, 493–521. [3](#)
- RATNAKUMAR, A., MOUSSET, S., GLÉMIN, S., BERGLUND, J., GALTIER, N., DURET, L. & WEBSTER, M. (2010). Detecting positive selection within genomes: the problem of biased gene conversion. *Philos Trans R Soc Lond B Biol Sci*, **365**, 2571–80. [9](#)
- SCHNEIDER, A., SOUVOROV, A., SABATH, N., LANDAN, G., GONNET, G. & GRAUR, D. (2009). Estimates of positive darwinian selection are inflated by errors in sequencing, annotation, and alignment. *Genome Biol Evol*, **1**, 114–8. [8](#), [9](#), [27](#)
- SMITH, S. & DONOGHUE, M. (2008). Rates of molecular evolution are linked to life history in flowering plants. *Science*, **322**, 86–9. [24](#)
- STORZ, J., HOFFMANN, F., OPAZO, J. & MORIYAMA, H. (2008). Adaptive functional divergence among triplicated alpha-globin genes in rodents. *Genetics*, **178**, 1623–38. [9](#)
- STUDER, R., PENEL, S., DURET, L. & ROBINSON-RECHAVI, M. (2008). Pervasive positive selection on duplicated and nonduplicated vertebrate protein coding genes. *Genome Res*, **18**, 1393–402. [9](#)

BIBLIOGRAPHY

- TEYTELMAN, L., OZAYDIN, B., ZILL, O., LEFRANÇOIS, P., SNYDER, M., RINE, J. & EISEN, M. (2009). Impact of chromatin structures on DNA processing for genomic analyses. *PLoS One*, **4**, e6700. [11](#)
- WANG, Y. & GU, X. (2001). Functional divergence in the caspase gene family and altered functional constraints: statistical analysis and prediction. *Genetics*, **158**, 1311–20. [9](#)
- WHELAN, S. & GOLDMAN, N. (2004). Estimating the frequency of events that cause multiple-nucleotide changes. *Genetics*, **167**, 2027–43. [28](#)
- YANG, Z. (2007). PAML 4: phylogenetic analysis by maximum likelihood. *Mol Biol Evol*, **24**, 1586–91. [19](#)